UC Davis
UC Davis Previously Published Works

Title

Additional Safety Assessments Needed for Diamide Insecticides

Permalink

Journal

Toxicological Sciences, 171(2)

ISSN

1096-6080

Authors

Pessah, Isaac N
Truong, Kim M

Publication Date

2019-10-01

DOI

10.1093/toxsci/kfz062

Peer reviewed

Interactions of Dichlorodiphenyltrichloroethane (DDT) and Dichlorodiphenyldichloroethylene (DDE) With Skeletal Muscle Ryanodine Receptor Type 1

Kim M. Truong, Gennady Cherednichenko, and Isaac N. Pessah[1]

Department of Molecular Biosciences, School of Veterinary Medicine, University of California, Davis, Davis, California 95616-5270

[1]To whom correspondence should be addressed at Department of Molecular Biosciences, School of Veterinary Medicine, University of California, Davis, 1089 Veterinary Medicine Drive, Davis, CA 95616. Fax: (530) 752-4698. E-mail: inpessah@ucdavis.edu.

ABSTRACT

Dichlorodiphenyltrichloroethane (DDT) and its metabolite dichlorodiphenyldichloroethylene (DDE) are ubiquitous in the environment and detected in tissues of living organisms. Although DDT owes its insecticidal activity to impeding closure of voltage-gated sodium channels, it mediates toxicity in mammals by acting as an endocrine disruptor (ED). Numerous studies demonstrate DDT/DDE to be EDs, but studies examining muscle-specific effects mediated by nonhormonal receptors in mammals are lacking. Therefore, we investigated whether o,p'-DDT, p,p'-DDT, o,p'-DDE, and p,p'-DDE (DDx, collectively) alter the function of ryanodine receptor type 1 (RyR1), a protein critical for skeletal muscle excitation-contraction coupling and muscle health. DDx (0.01–10 μM) elicited concentration-dependent increases in [^{3}H]ryanodine ([^{3}H]Ry) binding to RyR1 with o,p'-DDE showing highest potency and efficacy. DDx also showed sex differences in [^{3}H]Ry-binding efficacy toward RyR1, where [^{3}H]Ry-binding in female muscle preparations was greater than male counterparts. Measurements of Ca^{2+} transport across sarcoplasmic reticulum (SR) membrane vesicles further confirmed DDx can selectively engage with RyR1 to cause Ca^{2+} efflux from SR stores. DDx also disrupts RyR1-signaling in HEK293T cells stably expressing RyR1 (HEK-RyR1). Pretreatment with DDx (0.1–10 μM) for 100 s, 12 h, or 24 h significantly sensitized Ca^{2+}-efflux triggered by RyR agonist caffeine in a concentration-dependent manner. o,p'-DDE (24 h; 1 μM) significantly increased Ca^{2+}-transient amplitude from electrically stimulated mouse myotubes compared with control and displayed abnormal fatigability. In conclusion, our study demonstrates DDx can directly interact and modulate RyR1 conformation, thereby altering SR Ca^{2+}-dynamics and sensitize RyR1-expressing cells to RyR1 activators, which may ultimately contribute to long-term impairments in muscle health.

Key words: dichlorodiphenyltrichloroethane; dichlorodiphenyldichloroethylene; ryanodine receptors; skeletal muscle.

Although banned worldwide in the 1970s because of health and environmental issues, the organochlorine pesticide dichlorodiphenyltrichloroethane (DDT) and its metabolite dichlorodiphenyldichloroethylene (DDE) remain ubiquitous in the environment (Mansouri *et al.*, 2017; Sanger *et al.*, 1999). Through its unregulated use and owing to its high lipophilicity, which results in bioconcentration, DDT and even greater levels of DDE can still be detected in living organisms, mainly deposited in fat (Nicolopoulou-Stamati *et al.*, 2016; Patterson *et al.*, 2009; Rodriguez-Alcala *et al.*, 2015). Although the use and production

of DDT has been eliminated from most countries, the World Health Organization (WHO) has sanctioned the pesticide for indoor use as part of Integrated Vector Management to control vector-borne diseases such as malaria (EPA, 2017). Its environmental persistence in combination with improper disposal of legacy sources, exemplified by the Montrose, Del Amo and the Palos Verdes Superfund sites in Southern California, continue to contribute a heavy environmental burden of the pesticide and pose health risks even in the United States (Coffin *et al.*, 2017; Kucher and Schwarzbauer, 2017).

DDT exerts its insecticidal activity by binding to voltage-gated sodium channels on the axons of neurons in insects to stabilize its open state and to inhibit channel inactivation or de-activation (Coats, 1990; Narahashi, 2000; Silver et al., 2017; Zhorov and Dong, 2017). Toxicity studies demonstrate that high concentrations of DDT are required to mediate neurotoxicity in mammals (Silver et al., 2017), thus its endocrine disrupting properties have been more widely investigated. The original technical mixture of DDT consisted of a combination of both p,p′-DDT (77%) and o,p′-DDT (23%) with the latter recognized as the more estrogenic isomer (Baker and Lathe, 2018; Gellert et al., 1972; Kojima et al., 2004). One of its major and persistent metabolites, p,p′-DDE has also been identified as an endocrine disrupting compound (EDC), possessing anti-androgenic properties (Bornman et al., 2018; Kelce et al., 1995; Kojima et al., 2004; Patrick et al., 2016). Although numerous studies have demonstrated that both the parent compound and the metabolite are endocrine disruptors, and that DDT and DDE body burden increases with age in humans (Mnif et al., 2011; Turusov et al., 2002; Tyagi et al., 2015; Zumbado et al., 2005), studies examining mammalian organ-specific effects mediated by nonhormonal receptors have been lacking.

Our laboratory previously published an unexpected finding demonstrating that in addition to activating estrogen receptors (ESR), o,p′-DDE can also engage with the ryanodine receptor type 1 (RyR1) (Morisseau et al., 2009). Ryanodine receptors (RyRs) are homotetrameric Ca^{2+}-release channels broadly expressed on sarcoplasmic reticulum (SR) membranes of muscle and on the endoplasmic reticulum (ER) of non-muscle cells (Pessah et al., 2010). Mammals possess 3 RyR isoforms with RyR1 predominantly found in skeletal muscle. RyR1 is a critical component of excitation-contraction coupling (ECC) through its strict regulation of intracellular Ca^{2+} ($[Ca^{2+}]_i$) stores. Disruption of RyR1-signaling by anthropogenic chemicals, as observed with polychlorinated biphenyls (PCBs) and tetrabromobisphenol A (TBBPA), can lead to ECC dysfunction and/or impairments in skeletal muscle health (Niknam et al., 2013; Zhang and Pessah, 2017).

In our study, we conducted a more thorough examination of skeletal muscle-specific sequelae from exposure to each of the 4 relevant isomers—o,p′-DDT, p,p′-DDT, o,p′-DDE, and p,p′-DDE (collectively referred to as DDx). Our findings indicate that DDx can directly interact with and modulate skeletal muscle RyR1 conformation and sensitize RyR1 to activation in a RyR1 recombinantly expressed human embryonic kidney 293T (HEK293T) cell model. Similarly, o,p′-DDE heightens skeletal myotube sensitivity to electrical stimulation to mediate Ca^{2+}-transient amplitudes that are significantly larger than control-treated myotubes, and also accelerate muscle fatigability. Alterations in RyR1 function have been firmly established to be involved in the etiology of several aging related myopathic disorders in humans (Bellinger et al., 2008; Snoeck et al., 2015; Voermans et al., 2016), suggesting that long-term exposure to DDT and DDE might contribute to unhealthy muscle aging and impairments in muscle function.

MATERIALS AND METHODS

Chemicals. o,p′-DDT ($\geq$ 97.4%; CAS: 789-02-6), p,p′-DDT ($\geq$ 97.7%; CAS: 50-29-3), o,p′-DDE ($\geq$ 99.9%; CAS: 3424-82-6), p,p′-DDE (100%; CAS: 72-55-9) were obtained from AccuStandard (New Haven, Connecticut). [³H]Ryanodine (56.6 Ci/mmol) was obtained from PerkinElmer (Billerica, Massachusetts). Ryanodine ($\geq$ 98.3%; CAS: 15662-33-6) was obtained from Tocris

Bioscience (Minneapolis, Minnesota). Arsenazo III ($\geq$ 95%; CAS: 1668-00-4) was obtained from Santa Cruz Biotechnology (Dallas, Texas). Dithiothreitol (DTT; $\geq$ 98%; CAS: 3483-12-3) and 0.1 M calcium chloride solution (CAS: 10043-52-4) were purchased from Fisher Scientific (Waltham, Massachusetts). Nonfluorescent acetoxymethyl ester (Fluo-4 AM; $\geq$ 95%; CAS: 273221-67-3) was purchased from Invitrogen (Waltham, Massachusetts). The following were obtained from Sigma-Aldrich (St. Louis, Missouri): Bisphenol A ($\geq$ 99%; CAS 80-05-7), thapsigargin ($\geq$ 98%; CAS: 67526-95-8), adenosine 5′-triphosphate magnesium salt ($\geq$ 95%; CAS: 74804-12-9), phosphocreatine disodium salt hydrate ($\geq$ 97%; CAS: 19333-65-4), cyclopiazonic acid (CPA) ($\geq$ 98%; CAS: 18172-33-3), 1M magnesium chloride solution (CAS: 7786-30-3), ruthenium red (RR) ($\geq$ 85%; CAS: 11103-72-3), caffeine ($\geq$ 99%; CAS: 58-08-2), phenylmethylsulfonyl fluoride (PMSF; 98%; CAS: 329-98-6), leupeptin hydrochloride ($\geq$ 90%; CAS 24125-16-4), and type 1 creatine phosphokinase ($\geq$ 150 units/mg protein; CAS: 9001-15-4).

Animals. All collections of mouse and rabbit tissues for the studies were conducted using protocols approved by the Institutional Animal Care and Use Committee (IACUC) at the University of California at Davis (Davis, California).

Preparation of RyR1-enriched junctional sarcoplasmic reticulum membrane from rabbit muscles. RyR1-enriched junctional sarcoplasmic reticulum (JSR) membrane fractions were isolated from the back and hind limb skeletal muscles of wild-type male (1.5 kg) New Zealand White rabbits (Charles River, Hollister, California) as previously described in Pessah et al. (1986), Saito et al. (1984), and Truong and Pessah (2018) to investigate whether o,p′-DDT, p,p′-DDT, o,p′-DDE, or p,p′-DDE (DDx, collectively) trigger Ca^{2+} release from RyR1. Approximately 200 g of skeletal muscle tissue was flash frozen in liquid nitrogen, grounded into a fine powder with a mortar and pestle, and subsequently homogenized in a Waring blender for 1 min in aqueous homogenization buffer (pH 7.4) containing 300 mM sucrose, 5 mM imidazole, 100 μM PMSF, and 10 μg/ml leupeptin hydrochloride. The mixture was centrifuged at 5500 $\times$ g for 10 min. The supernatant was then removed and the pellet re-homogenized and recentrifuged. Supernatants were combined and filtered through a mesh sieve before being centrifuged at 110 000 $\times$ g for 1 h at 4°C. The supernatant was discarded and the pellet was homogenized with a glass Dounce in aqueous homogenization buffer before being transferred to the top of a discontinuous sucrose gradient (45%, 38%, 34%, 32%, and 27%, w/v in aqueous homogenization buffer). The gradient was centrifuged at 72 128 $\times$ g for 15 h at 4°C. Supernatant from the 38% and 45% fractions were pooled and diluted to 10% sucrose using an aqueous 5 mM imidazole buffer, and centrifuged at 110 000 $\times$ g for 1 h at 4°C. Final JSR pellets were resuspended in ice-cold aqueous buffer (pH 7.4) containing 300 mM sucrose and 10 mM HEPES, aliquoted, flash frozen, and stored at −80°C for either [³H]ryanodine ([³H]Ry) binding analysis or macroscopic Ca^{2+} flux assessments.

Membrane fraction preparations from mouse skeletal muscle. Crude membrane fraction from the skeletal muscle of 4- to 5-month-old individual male and female wild-type C57BL/6J mice (n = 8 per sex) was prepared as previously described in Truong and Pessah (2018). Limb skeletal muscles were flash frozen, grounded, and placed into ice-cold aqueous buffer (pH 7.4) containing (in mM) 300 sucrose, 10 HEPES, 10 μg/ml leupeptin hydrochloride, 0.1 PMSF, 10 sodium fluoride (NaF), 2 β-glycerophosphate, 0.5 mM sodium orthovanadate (Na₃VO₄), and

1.5 ethylene glycol tetraacetic acid (EGTA). The mixture was homogenized with 3 sequential bursts of 30 s at 10 000 RPM using a PowerGen 700 D (Thermo Fisher, Waltham, Massachusetts) and centrifuged at 90 × g for 1 min. The mixture was filtered, and the collected supernatant was centrifuged at 110 000 × g for 1 h at 4°C. Final pellets were resuspended in ice-cold aqueous buffer (pH 7.4) containing 300 mM sucrose and 10 mM HEPES, aliquoted, flash frozen, and stored at −80°C.

Protein concentration determination. Protein concentrations of all membrane protein preparations were determined using the Pierce BCA protein assay kit (Thermo Fisher). The kit was validated by utilizing our own albumin standard composed of precisely weighted bovine serum albumin (BSA) dissolved in water, in lieu of the albumin standard ampules available for purchase. Therefore, the exact concentration of protein in all created dilutions is known, and our laboratory can assess the standard curve to determine if there are any problems or concerns with the kit.

Macroscopic Ca^{2+} flux measurements. Net Ca^{2+} flux across JSR membrane vesicles were assessed in real time using metallochromic Ca^{2+} indicator dye arsenazo III (AsIII) as previously described in Feng *et al.* (2017) and Truong and Pessah (2018). JSR membrane vesicles at 100 µg/ml were added into 35°C cuvettes containing aqueous medium (pH 7.4) consisting of (in mM) 100 KCl, 6 sodium pyrophosphate, 0.25 AsIII, and 20 4-morpholine-propanesulfonic acid (MOPS), 2 Mg^{2+}ATP, 10 phosphocreatine, and 20 µg/ml creatine phosphokinase. JSR vesicles were loaded with Ca^{2+} by 3 sequential additions of $CaCl_2$ (45 nmol total) and then exposed to 0.1% DMSO (v/v) vehicle control or 10 µM o,p'-DDT, p,p'-DDT, o,p'-DDE, or p,p'-DDE to determine their ability to trigger Ca^{2+} leak. In a few experiments, 2 µM RR was added to the cuvette once Ca^{2+} leak was observed to completely block RyR1 leak, followed by addition of 50 µM CPA to completely inhibit SERCA (the SR/ER Ca^{2+} ATPase) activity. Calibration of AsIII signals at the end of each experiment was performed with stepwise addition of $CaCl_2$ from a National Bureau of Standard stock.

[^{3}H]Ry-binding analysis. Specific [^{3}H]Ry binding to either rabbit JSR membrane preparations or mouse skeletal muscle homogenates were measured as previously described in Pessah and Zimanyi (1991) and Truong and Pessah (2018). Rabbit JSR RyR1-enriched membrane preparations were used to establish concentration-effect curves for o,p'-DDT, p,p'-DDT, o,p'-DDE, and p,p'-DDE (DDx, collectively) to determine both efficacy and potency; whereas, mouse skeletal muscle microsomal preparations were used to increase power and to investigate sex differences in DDx potency toward RyR1. [^{3}H]Ry-binding protocols were the same for both preparations unless specified otherwise.

Rabbit JSR membrane or mouse microsomes (100 µg/ml) were incubated with ice-cold aqueous binding buffer (pH 7.4) containing (in mM) 140 KCl, 15 NaCl, 20 HEPES, and nominal free Ca^{2+} without EGTA buffering for binding of 5 nM [^{3}H]Ry under equilibrium assay conditions (3 h at 37°C) with constant shaking. Assays using JSR membranes were performed in the absence or presence of 10 µM BPA (negative control for RyR1 activity) (Zhang and Pessah, 2017), or an increasing concentration of DDx (0.01–100 µM). Assays using mouse microsomes were incubated in the absence or presence of 10 µM DDx with constant shaking. Nonspecific binding was determined by incubating with 1000-fold (5 µM) excess of

unlabeled ryanodine in the absence or presence of specified compound.

Bound ligand was separated from free ligand by filtration through Whatman GF/B glass fiber filters (Whatman, Clifton, New Jersey) using a model M-24 cell harvester (Brandel, Gaithersburg, Maryland) and washed thrice with 5 ml of ice-cold aqueous harvesting buffer (pH 7.4) consisting of (in mM) 140 KCl, 0.1 $CaCl_2$, and 10 HEPES. Filters were completely submerged in 4 ml of scintillation fluid (ScintiVerse BD Cocktail, Fisher Scientific, Waltham, Massachusetts) and [^{3}H]Ry trapped to the filter quantified using a Beckman Coulter LS6500 spectrometer (Beckman Coulter, Indianapolis, Indiana). Experiments with JSR membrane preparations were performed in triplicate ($n = 3$) and replicated with a different JSR membrane preparation with final DMSO concentration ≤ 1% (v/v). Membranes from 8 mice per sex were tested ($n = 8$ per sex), with each membrane run in triplicate. Specific radioligand binding in the presence of compound was normalized to percent DMSO vehicle control.

Western blot analysis of mouse skeletal muscle membrane preparations. To determine whether the observed sex difference in DDT and DDE potency toward RyR1 was due to differential RyR1 protein expression levels between the 2 sexes, western blots were performed on skeletal muscle membrane preparations from individual male or female wild-type C57BL/6 mice ($n = 7$ mice per sex). Samples were denatured in SDS-PAGE sample buffer (Bio-Rad, Hercules, California) containing 50 mM DTT. Skeletal protein (10 µg/lane) was loaded onto Novex precast 4%–12% gradient Tris-glycine gels (Thermo Fisher) and electrophoresed at 100 V for 15 min and then at 150 V for 2.5 h in aqueous NuPAGE MOPS SDS running buffer (Thermo Fisher). Proteins were transferred to methanol-activated polyvinylidene difluoride (PVDF) membranes (0.45 µm pore size; Bio-Rad) at 30 V for 15 h and then 150 V for 1.5 h. Membranes were blocked at room temperature with 10 ml Odyssey blocking buffer in PBS (LI-COR, Lincoln, Nebraska) for ≥ 1 h. The membranes were then incubated in primary antibodies diluted in blocking buffer containing 0.2% Tween-20 (v/v) overnight at 4°C with constant shaking. Total RyR1 was detected with the C34 antibody (Developmental Studies Hybridoma Bank, Iowa City, Iowa) at 1:500. The 12-kDa FK506-binding protein (FKBP12) was detected using the anti-FKBP12 antibody (Abcam, Cambridge, England) at 1:1000. The antibody for the housekeeping protein glyceraldehyde 3-phosphate dehydrogenase (GAPDH; Millipore, Billerica, Massachusetts) was diluted at 1:4000. After incubation with primary antibodies, the membranes were washed 6 times (10 min per wash) with Tris-buffered saline (TBS) containing 0.5% Tween-20 (v/v) and incubated with secondary antibodies diluted in blocking buffer and 0.2% Tween 20 (v/v) at a dilution of 1:10 000 for 1 h using either an 800 nm fluorescent-conjugated goat anti-mouse secondary (LI-COR), or a 700 nm fluorescent-conjugated goat anti-rabbit secondary (LI-COR). After incubation with the secondary antibodies, the membranes were washed 6 times (10 min per wash) with TBS containing 0.5% Tween-20 (v/v). Finally, the membranes were imaged using an Odyssey Infrared Imager (Li-COR) and densitometry analysis was performed using Image Studio Lite (Li-COR). RyR1 protein in all samples was proteolyzed, thus all immunopositive bands > 320 kDa were included in the densitometric analysis.

HEK293T cell maintenance. Human embryonic kidney 293T cells transfected to stably express wild-type RyR1 (HEK-RyR1) were previously established and validated in our laboratory (Barrientos *et al.*, 2009; Kim *et al.*, 2011; Pessah *et al.*, 2009) and stored in liquid nitrogen until needed. For the following

experiments, HEK293T cells were seeded onto uncoated 10-cm cell culture-treated dishes and maintained in maintenance medium (Dulbecco's modified Eagles medium [DMEM] supplemented with 2 mM glutamine, 100 μg/ml streptomycin, 100 U/ml penicillin, 1 mM sodium pyruvate, 0.5 μg/ml geneticin sulfate [G418], and 10% fetal bovine serum [FBS; v/v]; all purchased from Thermo Fisher), and kept at 37°C under 5% CO_2. Wild-type HEK293T cells (HEK-Null), which lack RyR1 expression, were kept under the same conditions except the selection antibiotic G418 was omitted from the media. A full media change was performed every other day. Cells were passaged onto new sterile 10-cm dishes when they reached approximately 80% confluency.

Compound preparation for Ca^{2+} imaging of HEK293T cells or differentiated skeletal primary myotubes. Grade 514 molecular sieves (Type 4 A; Thermo Fisher) were placed into 15 ml of DMSO for $\geq$ 24 h to remove all water molecules to create "dry" DMSO. Each DDT and DDE congener was then dissolved in dry DMSO at a stock concentration of 10 mM. A volume of the stock solution was further diluted with dry DMSO to create secondary stock solutions of 5, 1, and 0.1 mM. For Ca^{2+}-imaging assays of the acute effects of DDT or DDE, stock concentrations of DDT or DDE were diluted in Tyrode solution with the final DMSO concentration at 0.1% (v/v) for all chemicals. For Ca^{2+}-imaging assays of HEK293T cells to assess subchronic (12 or 24 h) effects, stock concentrations of DDT or DDE were diluted in DMEM supplemented with 2 mM glutamine, 100 μg/ml streptomycin, 100 U/ml penicillin, and 1 mM sodium pyruvate with the final DMSO concentration at 0.1% (v/v) for all chemicals; FBS was omitted to prevent the chemical from binding to albumin. For Ca^{2+}-imaging assays of differentiated skeletal myotubes to assess the subchronic effect (24 h) of the most potent DDx congener, o,p'-DDE, a stock concentration of o,p'-DDE was diluted in myotube differentiation media consisting of DMEM supplemented with 100 μg/ml streptomycin, 100 U/ml penicillin, and 5% heat-inactivated horse serum (HIHS; v/v) with the final DMSO concentration at 0.01% (v/v). HEK293T cells were incubated with the diluted chemical at 37°C under 5% CO_2 for 12 or 24 h depending on the assay. In contrast, differentiated myotubes were incubated with the diluted chemical at 37°C under 10% O_2/5% CO_2 for 24 h.

Calcium imaging of HEK293T cells. HEK-Null and HEK-RyR1 cells were used for Ca^{2+} imaging as previously described in Barrientos et al. (2009), Kim et al. (2011), and Pessah et al. (2009) to investigate whether o,p'-DDT, p,p'-DDT, o,p'-DDE, or p,p'-DDE directly engage with RyR1 to elicit Ca^{2+} leak. HEK-Null or HEK-RyR1 cells were seeded (50 000 cells per well) onto collagen coated 96-well clear-bottomed black imaging plates. Cells were placed back into the incubator at 37°C under 5% CO_2 to recover for 20 to 24 h. For acute studies or following subchronic treatment, all media were removed and the cells were loaded with 75 μl of 5 μM Fluo-4 AM dissolved in aqueous Tyrode solution (pH 7.4) containing (in mM) 125 NaCl, 5 KCl, 1.2 $MgCl_2$, 6 glucose, 25 HEPES, and 2 $CaCl_2$ supplemented with 0.5 mg/ml BSA for 60 min at 37°C. Dye loaded-cells were washed 4 times (225 μl per wash) with warm Tyrode solution leaving a final volume of 150 μl in each well. Cells were maintained at room temperature for an additional 15 min to allow for complete de-esterification of intracellular AM esters.

Once ready, the plate of cells was transferred into the Fluorescent Imaging Plate Reader (FLIPR TETRA) platform (Molecular Devices, San Jose, California) where the cells were excited at 488 nm and Ca^{2+}-bound Fluo-4 emission in the 500 nm range was recorded. Readings were taken once every second for 2 min to establish a baseline reading prior to addition of compound and for an additional 8–10 min following the addition of compound. For acute studies, 2 min of baseline was recorded before cells were treated with 10 μM of either DDT or DDE in the absence or presence of 100 μM caffeine. For some experiments, 100 μM caffeine was added to the cells following either baseline recording or at 100 s after addition of 10 μM DDT or DDE. For subchronic studies, 2 min of baseline was recorded before addition of 100 μM caffeine.

Preparation and single cell calcium imaging of differentiated primary skeletal myotubes. Primary skeletal myoblasts were isolated from mixed-sex neonatal wild-type C57BL6 mice as previously established (Cherednichenko et al., 2008; Zhang and Pessah, 2017). The myoblasts were grown in maintenance media composed of Ham's F10 medium, 20% bovine growth serum (BGS; v/v), 100 μg/ml streptomycin, 100 U/ml penicillin, and supplemented with 5 ng/ml basic fibroblast growth factor (FGF; PeproTech, Inc; Rocky Hill, New Jersey) on collagen-coated 10-cm cell culture-treated dishes (Costar, Cambridge, Massachusetts) at 37°C under 10% O_2/5% CO_2. A half media change was performed daily, and cells were passaged onto new sterile collagen-coated 10-cm dishes when they reached approximately 60% confluency or when required for Ca^{2+} imaging experiments.

For Ca^{2+} imaging experiments, myoblasts were seeded onto Matrigel (BD Biosciences; Franklin Lakes, New Jersey) coated clear bottomed black walled 96-well plates in the presence of myoblast maintenance media. Upon reaching approximately 60% confluency, all media were replaced with differentiation media consisting of DMEM supplemented with 100 μg/ml streptomycin, 100 U/ml penicillin, and 5% HIHS (v/v) for 2 days to allow for differentiation into myotubes. On day 2, the myotubes are pretreated for 24 h with either DMSO vehicle control or o,p'-DDE diluted in differentiation media and placed back into the 37°C incubator under 10% O_2/5% CO_2 for an additional 24 h. On day 3 or 24-h post-treatment, the differentiated primary myotubes undergo Ca^{2+} imaging as previously described in Cherednichenko et al. (2012), Gach et al. (2008), and Niknam et al. (2013), to investigate whether the most potent DDx congener, o,p'-DDE, affected ECC.

Differentiated mouse myotubes were treated with 1 μM o,p'-DDE for 24 h before the cells were loaded with 5 μM Fluo-4 AM for 20 min at 37°C in imaging buffer (pH 7.4) composed of (in mM) 125 NaCl, 5 KCl, 1.2 $MgCl_2$, 2 $CaCl_2$, 6 glucose, and 25 HEPES supplemented with 0.5 mg/ml BSA. The cells were then washed 3 times with the imaging buffer and then transferred to a Nikon microscope (Tokyo, Japan). Fluo-4 was excited at 488 nM using a DeltaRam excitation source (Photon Technology International; PTI, Lawrenceville, New Jersey), and fluorescence emission was measured at 516 nm using a Nikon 40× objective. Data were collected with a Cascade 512B charge-coupled device camera (Photometrics; Tucson, Arizona) from regions consisting of approximately 10–20 individual cells. Electrical field stimuli were applied using 2 platinum electrodes fixed to opposing sides of the well and connected to a Master-8 programmable pulse stimulator (AMPI; Jerusalem, Israel) set at 7 V, 1 ms bipolar pulse duration (0.5 ms each direction) over 1–20 Hz (10 s pulse train duration) to study the frequency-transient amplitude relationship. Some of the vehicle control and o,p'-DDE pretreated myotubes were also subjected to a well-established fatigue protocol (Gach et al., 2008) to examine the effect of DDx on fatigability (Refer to Supplementary information). All images were acquired
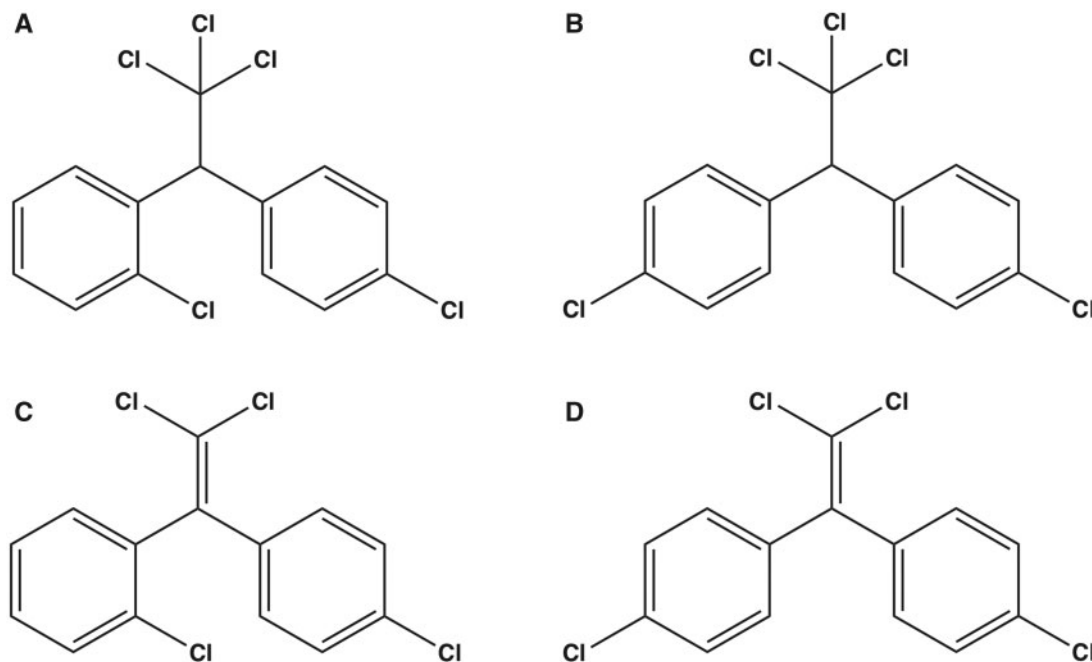
Figure 1. The chemical structures of both dichlorodiphenyltrichloroethane (DDT) and dichlorodiphenyldichloroethylene (DDE) congeners: (A), o,p′-DDT; B, p,p′-DDT; (C), o,p′-DDE; (D), p,p′-DDE.

using the PTI Easy Ratio Pro Software (Horiba; Kyoto, Japan). Ca^{2+} transients were normalized to baseline (F_0) of each cell and corrected for background. All experiments were replicated at least twice using 2 different passages, and all responding cells were used for analysis.

Statistical analysis. GraphPad Prism 7 software (La Jolla, California) was used to make comparisons using a 1-way ANOVA with either a Tukey's *post hoc* test or a Dunnett's *post hoc* test, or a Student's *t*-test, where appropriate ($^*p < .05$; $^{**}p < .01$; $^{***}p < .001$). GraphPad Prism 7 was also used to generate linear regression traces to determine Ca^{2+} release rate, and for nonlinear curve-fitting to determine EC_{50}-values and maximum response. All error bars represent standard deviation (SD) unless stated otherwise. Statistical analyses used for each data set are described in the figure legends.

RESULTS

DDT and DDE Enhance [³H]Ry-binding to RyR1 in a Concentration-dependent Manner. Both DDT isomers and both DDE isomers (o,p′-DDT, p,p′-DDT, o,p′-DDE, and p,p′-DDE; DDx, collectively) (Figs. 1A–D) were tested to determine their ability to enhance binding of [³H]Ry to RyR1-enriched JSR membrane preparations in the presence of low nanomolar concentration of [³H]Ry. Allosteric modulation of RyR conformation mediated by pharmacological or toxicological agents has been widely investigated with the use of low nanomolar [³H]Ry due to its ability to bind to the open state of RyR (Morisseau *et al.*, 2009; Truong and Pessah, 2018). All 4 DDx compounds stimulated [³H]Ry binding in a concentration-dependent manner with o,p′-DDE exhibiting greatest apparent potency (EC_{50}) and efficacy (maximum binding) (Figure 2). Although the maximum response mediated by the 4 DDx were significantly different from one another ($p = .001$), potency was only significantly different between the parent compound DDT and its metabolite DDE but not between isomers (ie,
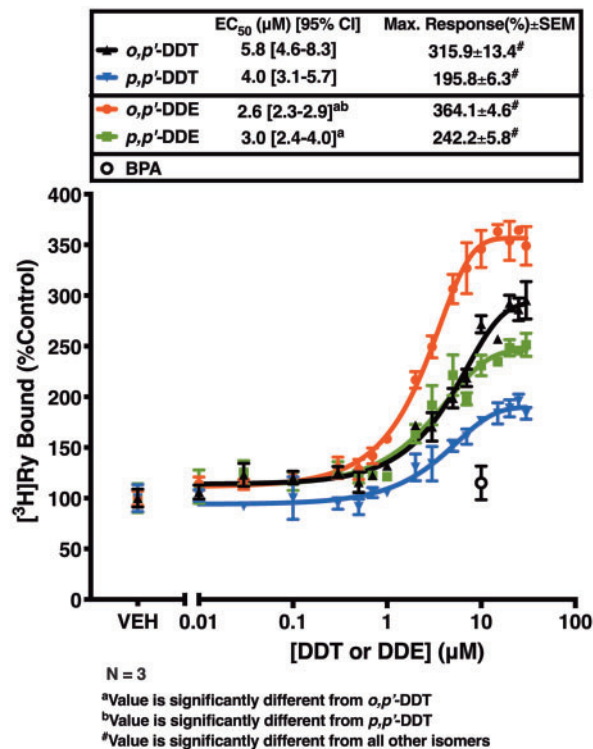
	EC_{50} (µM) [95% CI]	Max. Response(%)±SEM
o,p′-DDT	5.8 [4.6-8.3]	315.9±13.4[#]
p,p′-DDT	4.0 [3.1-5.7]	195.8±6.3[#]
o,p′-DDE	2.6 [2.3-2.9][ab]	364.1±4.6[#]
p,p′-DDE	3.0 [2.4-4.0][a]	242.2±5.8[#]
BPA		

N = 3

[a]Value is significantly different from o,p′-DDT
[b]Value is significantly different from p,p′-DDT
[#]Value is significantly different from all other isomers

Figure 2. Concentration-response curves for o,p′-DDT (triangle trace), p,p′-DDT (inverted triangle trace), o,p′-DDE (circle trace), and p,p′-DDE (square trace) with 10 µM bisphenol A (BPA; open circle) as a negative control. The maximum response is significantly different among all 4 congeners ($^{***}p < .001$). EC_{50}-values are significantly different between the parent compound DDT and its metabolite DDE, but not between congeners within the same group (ie o,p′-DDT vs p,p′-DDT). EC_{50}-values and maximum response were analyzed using a one-way ANOVA with Tukey *post hoc* test. Two different rabbit JSR membrane preparations were tested, with each membrane run in triplicate ($n = 3$).
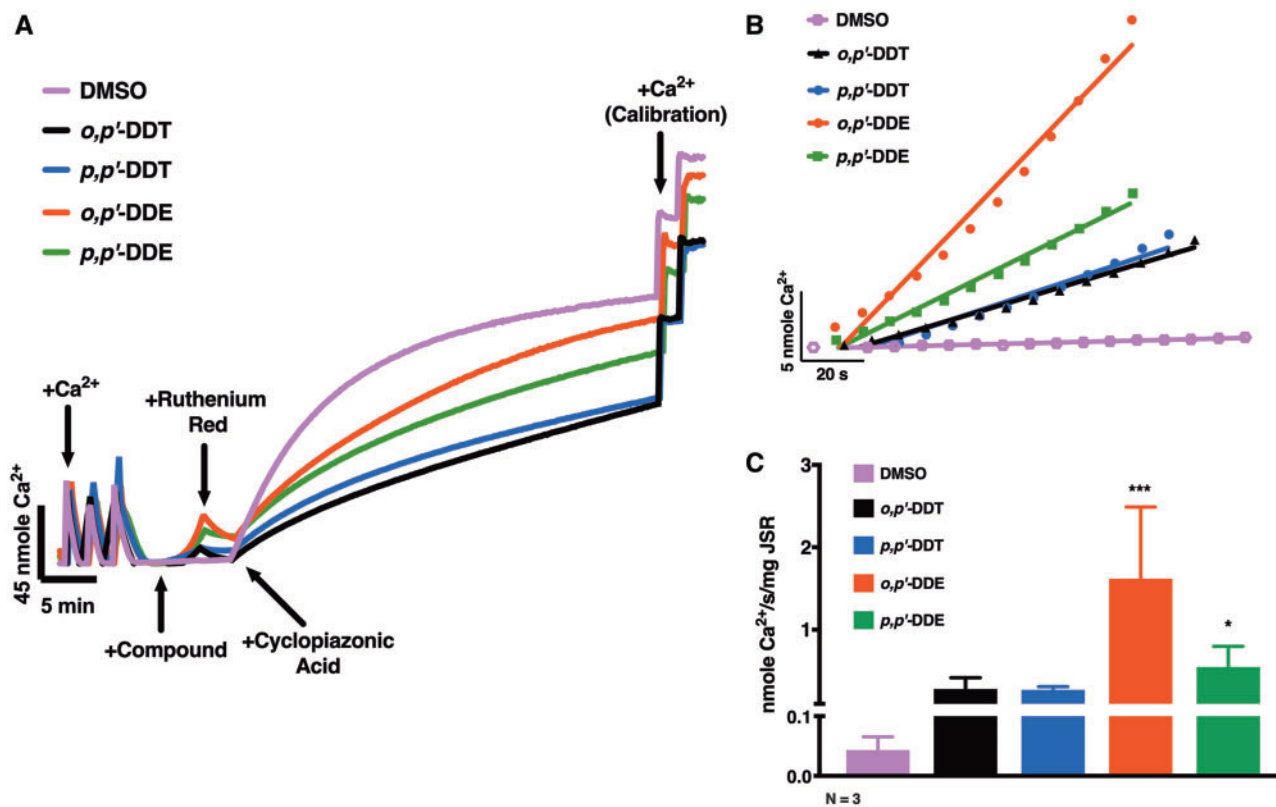
Figure 3. Both of the dichlorodiphenyltrichloroethane (DDT) and the dichlorodiphenyldichloroethylene (DDE) congeners potentiate Ca^{2+} release from sarcoplasmic reticulum (SR) stores through direct interaction with ryanodine receptor type 1 (RyR1). (A), Representative traces detailing the macroscopic Ca^{2+} efflux assay: rabbit junctional sarcoplasmic reticulum (JSR) vesicles were actively loaded with Ca^{2+} to near maximal capacity and then exposed to either 0.1% DMSO (v/v) vehicle control, 10 μM o,p'-DDT, 10 μM p,p'-DDT, 10 μM o,p'-DDE, or 10 μM p,p'-DDE. Following DMSO or DDx addition, 2 μM ruthenium red, a ryanodine receptor blocker, was added to determine if DDxmediated Ca^{2+} release by direct interaction with RyR1. Lastly, 50 μM cyclopiazonic acid, a sarco/endoplasmic reticulum Ca^{2+}-ATPase inhibitor, was added to prevent Ca^{2+} reuptake to allow for calibration of Ca^{2+}. (B) The initial 60 s of the Ca^{2+} release trace for DMSO vehicle control (square trace), o,p'-DDT (triangle trace), p,p'-DDT (inverted triangle trace), o,p'-DDE (circle trace), or p,p'-DDE (square trace) was assessed with a linear regression to determine Ca^{2+} release rate (nmole Ca^{2+}/s/mg JSR). (C), o,p'-DDE (37-fold) and p,p'-DDE (13-fold) significantly increased the rate of Ca^{2+} efflux from Ca^{2+}-loaded RyR1 SR vesicles compared with baseline leak rate, whereas both DDT congeners triggered a 6.5-fold difference. Three independent measurements replicated 3 times ($n = 3$) from different rabbit JSR preparations under identical condition were summarized and plotted (***$p < .001$; *$p < .05$, one-way ANOVA with Tukey *post hoc* test).

o,p'-DDT vs p,p'-DDT) (Figure 2). DDT and DDE with chlorine at the ortho position exhibited approximately 1.5- to 2.5-fold greater efficacy than their counterpart with both chlorines at the para position.

DDT and DDE Trigger Ca^{2+} Efflux From Microsomal Vesicles by Selective Interaction With RyR1. Due to the observed significant differences in the efficacy of the DDx compounds using our [³H]Ry-binding assay—where maximum response is achieved for each compound at approximately 10 μM—we tested the hypothesis that DDx directly engages with RyR1 to facilitate Ca^{2+} leak. We measured the ability of each compound at 10 μM to elicit Ca^{2+} efflux across RyR1-enriched vesicles in the presence of sarco/endoplasmic reticulum Ca^{2+}-ATPase (SERCA) activity using a well-established macroscopic Ca^{2+} transport assay (Figure 3). JSR membrane vesicles accumulated Ca^{2+} through active SERCA activity, and were then exposed to 10 μM DDx or 0.1% DMSO (v/v) vehicle control (Figure 3A). Both DDT isoforms elicited a similar moderate rate of net Ca^{2+} efflux from JSR vesicles, which was 6.5-fold greater than basal leak rate, whereas, o,p'-DDE and p,p'-DDE elicited a much more significant initial rate of Ca^{2+} efflux (37-fold and 13-fold, respectively) (Figs. 3B and C). Similar to what was observed with the [³H]Ry-binding assay, the DDE isoforms are more potent than their parent DDT isoforms. Addition of RR, an RyR blocker,

immediately mitigated Ca^{2+} efflux allowing for rapid Ca^{2+} accumulation by SERCA, reaffirming that (1) DDx-triggered efflux was mediated by direct interaction with RyR1, and (2) DDx has negligible effect on SERCA pump activity (Figure 3A).

DDT and DDE Potency Toward [³H]Ry-binding to RyR1 Show Sex Differences. The efficacy of DDx was reassessed in our [³H]Ry-binding assay using mouse skeletal muscle preparations in an effort to increase statistical power and to investigate possible differences between sexes (Figure 4A). DDx at 10 μM, the concentration previously observed to show maximal or near maximal response in the concentration-response curves using the [³H]Ry-binding assay (Figure 2), significantly increased [³H]Ry-binding to RyR1 as observed with JSR fractions (Figure 4A). Microsomal membranes from mice gave similar trends with o,p'-DDE and p,p'-DDT showing the highest and the lowest efficacies, respectively, with results pooled from both sexes (Figure 4A). However, maximum binding for p,p'-DDE was higher with the crude murine preparation compared with JSR, and comparable with that of o,p'-DDT.

As expected, [³H]Ry-binding analysis of either female preparations or male preparations showed the same trends in DDx-mediated maximum response in [³H]Ry-binding to RyR1: o,p'-DDE > p,p'-DDE > o,p'-DDT > p,p'-DDT (Figs. 4B and C).
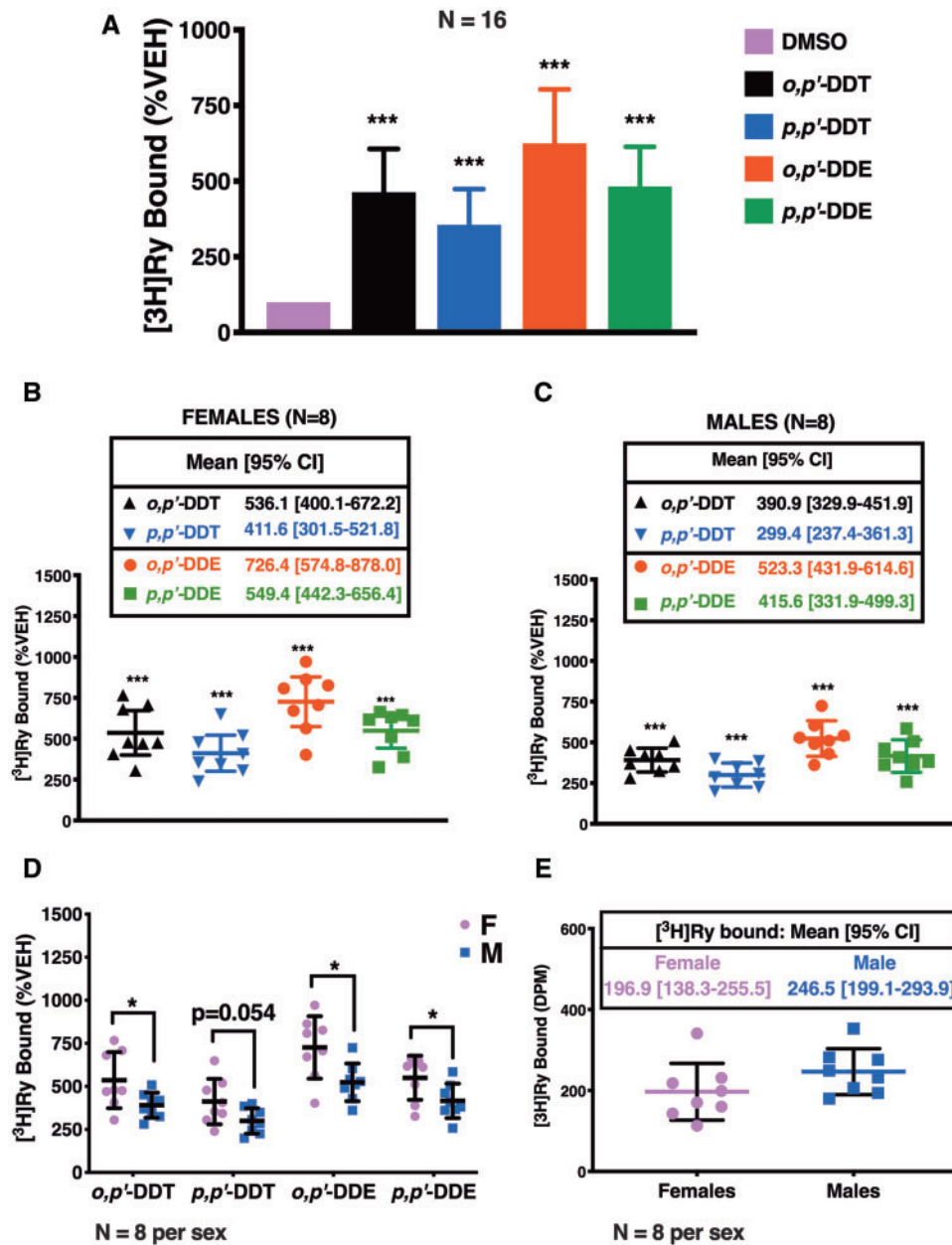
Figure 4. Mouse microsomal preparations from females are more sensitive to [³H]Ry-binding elicited by both dichlorodiphenyltrichloroethane (DDT) and dichlorodiphenyldichloroethylene (DDE) congeners at 10 μM compared with mouse microsomal preparations from males. (A), o,p′-DDT, p,p′-DDT, o,p′-DDE, and p,p′-DDE increased [³H]Ry-binding 3.5- to 6.5-fold higher than 0.1% DMSO (v/v) vehicle control. The same trend on the effects of the DDT and DDE congeners on [³H]Ry-binding was observed when (B) preparations from females (n = 8) were analyzed separately from (C) preparations from males (n = 8). (D) Both DDT and DDE congeners produced a significantly greater effect on [³H]Ry-binding to RyR1 with the preparations from females compared with the preparations from males, which was not attributed to differences in (E) total [³H]Ry basal binding. Experiments were performed in triplicate using 8 membrane preparations per sex from individual mice (n = 8 per sex). Statistical comparison of the effect of DDT and DDE congeners to DMSO vehicle control was performed with a one-way ANOVA with Tukey *post hoc* test, whereas, comparisons between the effect on the 2 sexes were performed with a Student's *t*-test (***p < .001; *p < .05).

However, DDx increased [³H]Ry-binding in preparations from female mice significantly more than in preparations from male mice across most of the isoforms, with p,p′-DDT trending toward significance (Figure 4D). The observed significant sex difference in DDT and DDE potency toward [³H]Ry-binding was not a result of differences in basal [³H]Ry-binding (Figure 4E). The preparations from the individual male and female mice were also assessed by western blotting to determine whether the observed sex differences were due to differential RyR1 expression levels or changes in accessory protein FK506-binding protein

(FKBP12), a protein well known to modulate RyR conformation (Jones et al., 2005; Ozawa, 2010) (Figure 5A). Proteolysis of RyR1 protein is typically observed with crude mouse skeletal muscle preparations and less so in more purified JSR preparations (Supplementary Figure 1). Therefore, western blot analysis was performed in 2 ways: (1) all immunopositive bands > 320 kDa were included in the densitometric analysis or (2) the densitometry of each band was analyzed separately and compared between sexes; the latter analysis showed no significant difference between the 2 sexes (data not shown). Overall, the
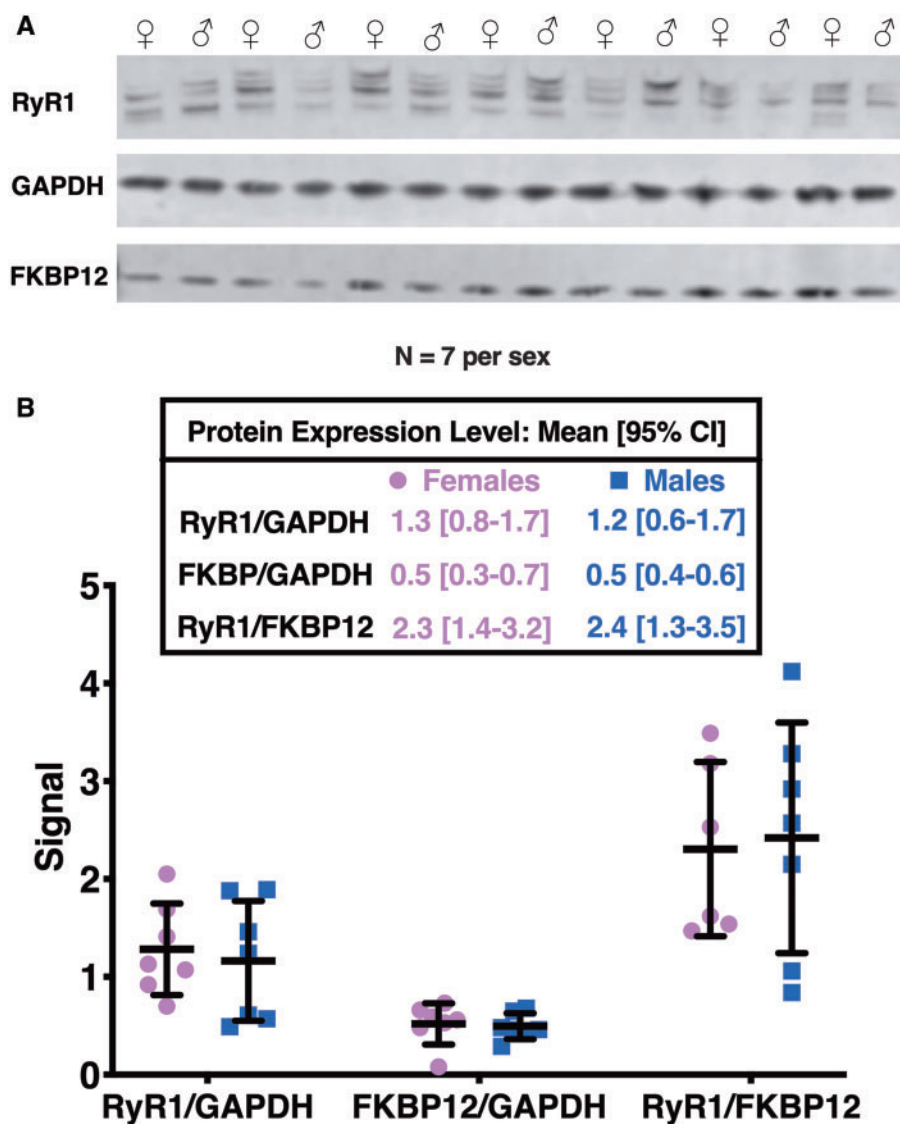
Figure 5. Neither FK506-binding protein (FKBP12) nor ryanodine receptor type 1 (RyR1) protein expression levels are different between preparations from female mice and preparations from male mice. (A), RyR1 microsomal preparations from individual female mice ($n = 7$) and individual male mice ($n = 7$) were assessed. (B), Densitometry analysis and a Student's t-test confirmed no significant differences in protein expression levels of FKBP12, RyR1, or the ratio of RyR1 to FKBP12 between the 2 sexes.

levels of protein expression for RyR1 and FKBP12 were similar between female and male mouse preparations (Figure 5B). The ratio of RyR1 expression to FKBP12 expression was also similar between the 2 sexes (Figure 5B). Ultimately, our results suggest inherent sex differences in DDx potency toward [³H]Ry-binding.

DDT and DDE Sensitize Caffeine-triggered Ca²⁺ Release in HEK293T Cells Stably Expressing RyR1. To assess whether the DDx isomers sensitize RyR1 in intact cells, HEK293T cells stably expressing human wild-type RyR1 receptors (HEK-RyR1) and wild-type HEK293T cells that do not express endogenous RyR1 (HEK-Null) were exposed to either an increasing concentration of DDx (0.1–10 μM) or 10 μM DDx, depending on the experiment. Cells were then loaded with the Ca²⁺ indicator dye Fluo-4 and their response to 100 μM caffeine measured using a high-throughput fluorescent imaging platform. Acute exposure to 0.1% DMSO (v/v) or 10 μM DDx, alone, did not affect HEK-RyR1 or HEK-Null cell

responses to the RyR agonist, caffeine (Figure 6A). Addition of 100 μM caffeine stimulated RyR1-mediated Ca²⁺ release from HEK-RyR1 cells but not HEK-Null cells (Figure 6A). Treatment of HEK-Null cells with 10 μM thapsigargin, a noncompetitive inhibitor of SERCA, caused rapid Ca²⁺ efflux from ER stores, which further confirmed the lack of response to caffeine in HEK-Null cells was solely due to lack of RyR1 protein expression and not due to impairment of the Ca²⁺ store (Figure 6B).

HEK-RyR1 cells and HEK-Null cells were acutely exposed to 100 μM caffeine in combination with 10 μM DDx to determine if DDx sensitizes RyR1. DDx in combination with caffeine elicited the same response as treatment with 0.1% DMSO (v/v) vehicle control (Figs. 7A, C, and E). However, addition of 10 μM DDx 100 s prior to addition of 100 μM caffeine significantly increased caffeine response in HEK-RyR1 cells as assessed by the amplitude and the area under the curve (AUC) of the transient (Figs. 7B, D, and F). Pretreatment with DDx for longer periods of
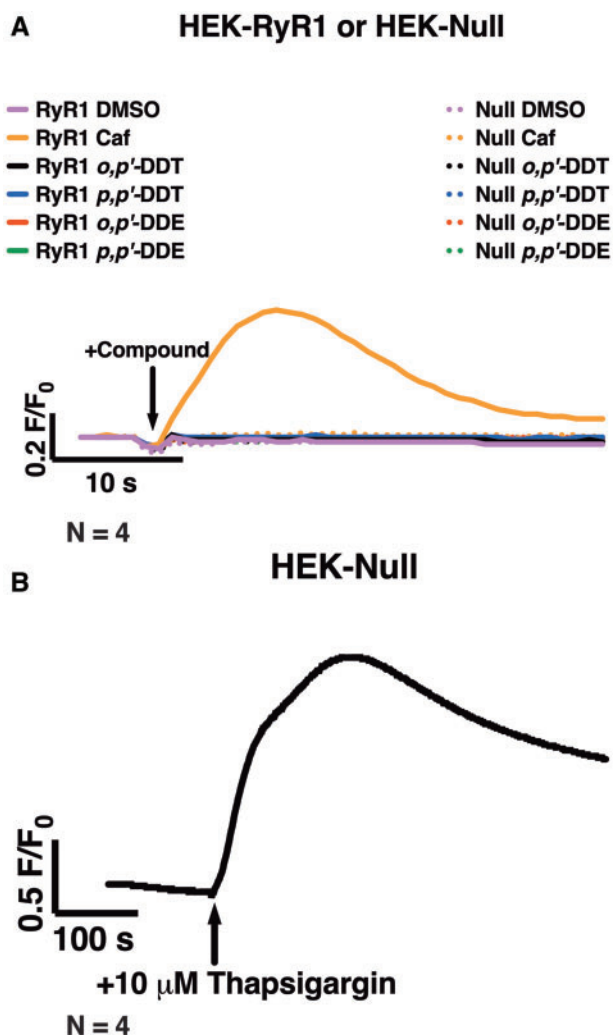
Figure 6. Acute treatment with either dichlorodiphenyltrichloroethane (DDT) or dichlorodiphenyldichloroethylene (DDE) congeners failed to mediate Ca^{2+} release from ryanodine receptor type 1 (RyR1)-expressing HEK293T cells (HEK-RyR1). (A and B), Fluo-4 fluorescence emission traces showing Ca^{2+}-transient responses of HEK-RyR1 cells and wild-type HEK293T cells (HEK-Null) to treatment with various compounds. (A), Immediate addition of 10 μM o,p'-DDT, 10 μM p,p'-DDT, 10 μM o,p'-DDE, 10 μM p,p'-DDE, or 0.1% DMSO (v/v) vehicle control did not facilitate Ca^{2+} release from HEK-RyR1 cells or HEK-Null cells; whereas, addition of 100 μM caffeine, an RyR1 agonist, stimulated Ca^{2+} release from stores in HEK-RyR1 cells but not HEK-Null cells. (B), Treatment of HEK-Null cells with 10 μM thapsigargin, a noncompetitive inhibitor of SERCA, mediated Ca^{2+} release from stores. Experiments were performed in sextuplicate and repeated 4 times ($n = 4$).

time increased DDx-mediated RyR1-sensitization to caffeine in a concentration- and time-dependent manner.

HEK-RyR1 cells pretreated with an increasing concentration of DDx (0.1–10 μM) for 12 h and then challenged with 100 μM caffeine showed increase in RyR1-sensitization in a concentration-dependent manner with 0.1–5 μM of DDx, and slower reaccumulation of Ca^{2+} into ER stores with 10 μM DDx (Figure 8A). Although 0.1–10 μM DDx exhibited a biphasic effect on the measured amplitude of the caffeine response, both DDT isomers at 10 μM increased the AUC (Figs. 8A and C). In contrast, DDE isomers at 10 μM, while similarly exhibiting a slower rate of Ca^{2+} reuptake into ER stores as observed with treatment with the parent compound DDT, decreased both the amplitude and AUC

of the caffeine response (Figs. 8A and C). Pretreatment of HEK-RyR1 cells with 0.1–10 μM DDx for 24 h increased RyR1 sensitization to caffeine responses in a concentration-dependent manner, with 5 and 10 μM DDx significantly increasing both the amplitude and AUC of the caffeine response compared with DMSO vehicle control (***$p < .001$) (Figs. 9A and B). In contrast to 12h DDx pretreatment, pretreatment with DDx for 24h facilitated the same monophasic increase in both amplitude and AUC of the caffeine response, thus only 1 parameter is shown (Figure 9B). Control western blot analysis confirmed stable expression of RyR1 protein on HEK-RyR1 cells and not HEK-Null cells, which further established the effects of DDT on caffeine-mediated response observed in HEK-RyR1 cells was mediated by selective interaction with RyR1 (Supplementary Figure 1).

Myotubes Pretreated With o,p'-DDE Hastens Fatigability and Heightens Sensitivity to Electrical Stimulation. To determine if DDx can selectively engage with RyR1 to disrupt Ca^{2+} dynamics and potentially mediate functional impairments in skeletal muscle, primary skeletal myotubes that endogenously express RyR1 were exposed to o,p'-DDE, the most potent congener of the 4 DDx. Myotubes were pretreated with o,p'-DDE at 1 μM for 24 h, the lowest concentration and the optimal pretreatment duration demonstrated to significantly sensitize RyR1 to caffeine in HEK-RyR1 cells compared with control cells, and allow sufficient time for o,p'-DDE to penetrate the cell membrane to reach intracellular targets, respectively (Figure 9).

Myotubes pretreated with vehicle control or 1 μM o,p'-DDE both exhibited ECC when electrically stimulated, displaying an increase in Ca^{2+}-transient amplitude in parallel with increasing electrical stimulation frequency. However, pretreatment with o,p'-DDE consistently enhanced Ca^{2+}-transient amplitude across all tested electrical stimulation frequencies when compared with vehicle-treated myotubes, with 1 Hz and $\geq$ 10 Hz facilitating a significant difference ($p \leq$ .05; Figure 10). As previously demonstrated, DMSO vehicle control pretreated myotubes challenged with the fatigue protocol were resistant to rundown (Gach *et al.*, 2008), but in contrast, o,p'-DDE pretreated myotubes displayed 2 qualitatively different patterns of impairment of electrically stimulated Ca^{2+} transients categorized as Type 1 and Type 2 (Supplementary Figure 2). Similar to the control group, the Type 1 group was resistant to rundown, but they consistently failed to produce the large initial overshoot in the first Ca^{2+}-transient typical of healthy myotubes at the time the fatigue stimulus protocol is initiated (Supplementary Figure 2). The Type 2 group demonstrated enhanced fatigability that invariably resulted in Ca^{2+}-transient instability and frequent failures throughout the fatigue stimulation protocol (Supplementary Figure 2).

DISCUSSION

Although the use of the organochlorine pesticide DDT has been banned worldwide except in extenuating circumstances, it can still be ubiquitously found in the environment due to its chemical stability and continued use to limit vector-borne-disease-carrying insects (Mansouri *et al.*, 2017; Sanger *et al.*, 1999). The WHO sanctions DDT use in tropical countries where vector-borne diseases, in particular malaria, threatens millions of people annually (Mansouri *et al.*, 2017; Mendes *et al.*, 2016; van den Berg *et al.*, 2017). Anthropogenic persistent organic pollutants such as DDT, and its more persistent metabolite DDE, are highly stable, highly lipophilic with a log Kow of 7, and recognized to rapidly and readily bioconcentrate in the environment and bioaccumulate in living organisms (Coffin *et al.*, 2017; Mansouri *et al.*, 2017; Nicolopoulou-Stamati *et al.*, 2016). DDT and DDE are well-recognized EDC, exhibiting
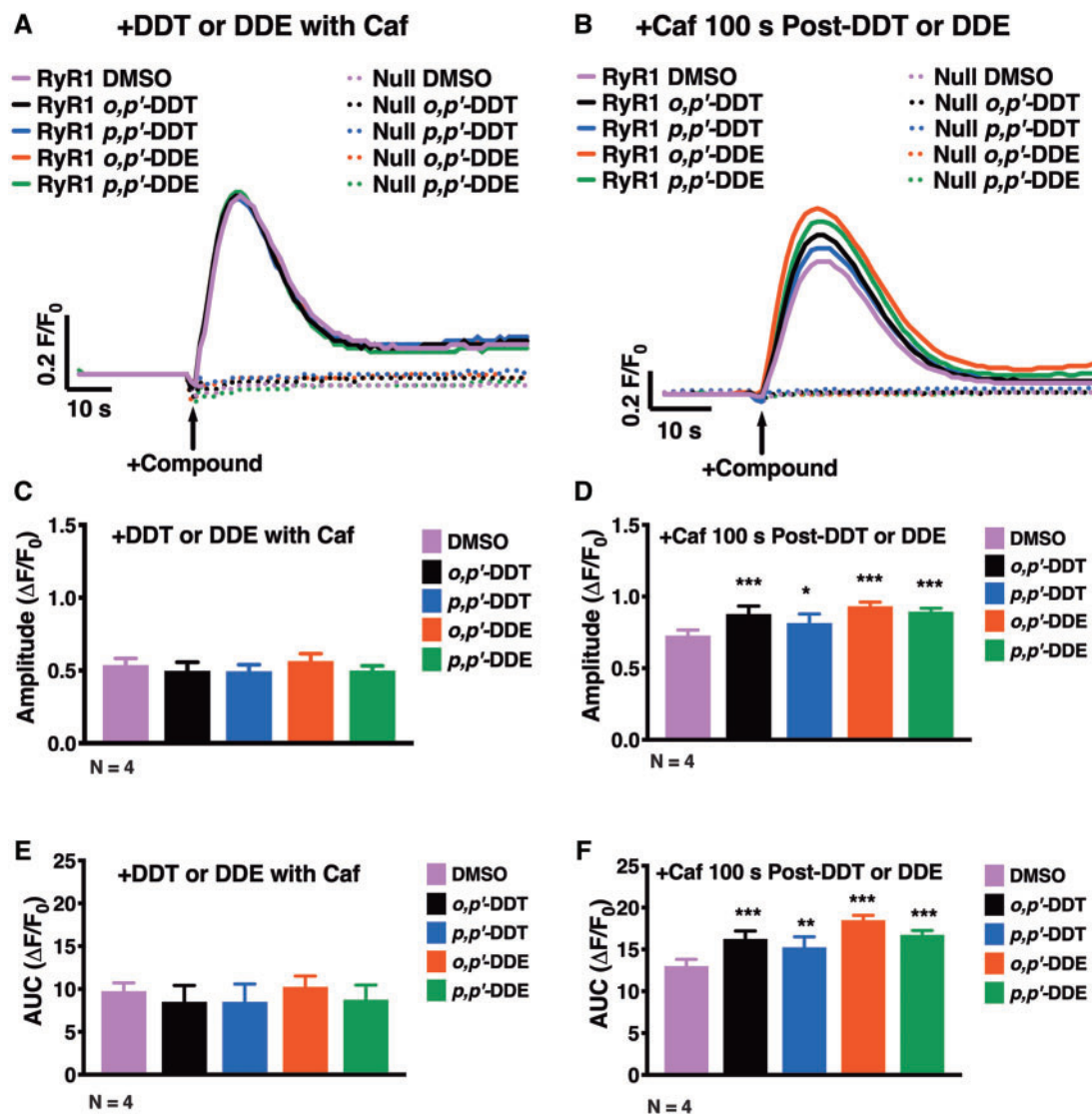
Figure 7. Dichlorodiphenyltrichloroethane (DDT) and dichlorodiphenyldichloroethylene (DDE) require time to permeate HEK-RyR1 cells to sensitize ryanodine receptor type 1 (RyR1) receptors. (A and B), Fluo-4 fluorescence emission traces showing Ca^{2+}-transient responses of HEK-RyR1 cells and HEK-Null cells. (A), Although addition of 100 μM caffeine simultaneously with 10 μM o,p'-DDT, p,p'-DDT, o,p'-DDE, p,p'-DDE, or 0.1% DMSO (v/v) vehicle control does not cause Ca^{2+} release from HEK-Null cells, it stimulates Ca^{2+} release from HEK-RyR1 cells. The degree of RyR1-stimulation by the congeners showed no significant differences compared with DMSO vehicle control as assessed by (C) amplitude and (E) area under the curve (AUC) post-activation. (B), However, addition of 10 μM of either DDT or DDE congener 100 s before addition of 100 μM caffeine sensitized RyR1 to the activating effect of 100 μM caffeine, increasing the (D) amplitude and (F) AUC post-stimulation, significantly compared with DMSO vehicle control with caffeine. Experiments were performed in triplicate and repeated 4 times ($n = 4$). Statistical comparison of the effect of DDT and DDE congeners to DMSO vehicle control was performed with a one-way ANOVA with Dunnett *post hoc* test (*$p < .05$; **$p < .01$; ***$p < .001$).

estrogenic and/or anti-androgenic properties (Baker and Lathe, 2018; Kelce *et al.*, 1995; Kojima *et al.*, 2004). We previously published a finding that confirmed o,p'-DDE activates ESRs, and also presented the novel data indicating that it can bind to skeletal muscle RyR1 (Morisseau *et al.*, 2009).

In this study, we conducted a systematic assessment of o,p'-DDE, and its 3 isomers, o,p'-DDT, p,p'-DDT, and p,p'-DDE, to determine whether they (1) interact with and modulate RyR1 conformation, (2) interact directly with RyR1 to mediate Ca^{2+} efflux, and (3) facilitate the same effect(s) on RyR1-signaling in cells. All 4 isomers, o,p'-DDT, p,p'-DDT, o,p'-DDE, and p,p'-DDE (collectively referred to as DDx) increased [³H]Ry-binding to RyR1 in a concentration-dependent manner with o,p'-DDE showing the highest potency and efficacy. Because [³H]Ry binds

to the open conformation of RyRs, our findings suggest that all DDx isomers interact with RyR1 to stabilize the ion channel in its open conformation. Our Ca^{2+} transport assay confirmed that DDx directly engaged with RyR1 to promote Ca^{2+} efflux from SR stores in the presence of strong SERCA pump activity, which acts in opposition of RyR1 activity.

DDx potency toward [³H]Ry-binding to RyR1 exhibited a small but statistically significant sex difference with DDx increasing [³H]Ry-binding to RyR1 more in preparations from female mouse skeletal muscle compared with those prepared from males. Although little is known regarding sex-dependent regulation of RyR1, 2 recent publications identified sexual dimorphisms in RyR-mediated hyperalgesic priming: ryanodine-induced priming in female rats was much greater than
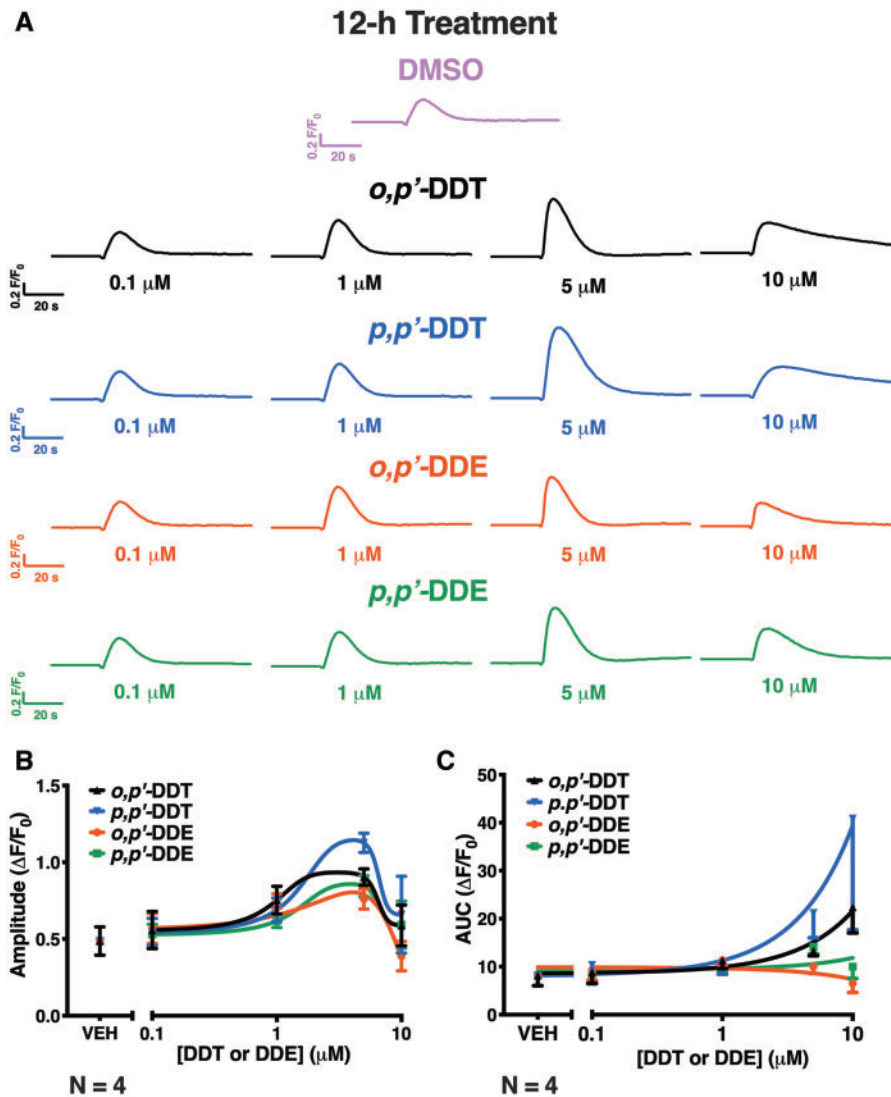
Figure 8. Pretreatment of HEK-RyR1 cells with either dichlorodiphenyltrichloroethane (DDT) or dichlorodiphenyldichloroethylene (DDE) congener for 12-h facilitated a biphasic effect on ryanodine receptor type 1 (RyR1)-sensitization to caffeine response. (A), Ca^{2+}-transient response mediated by addition of 100 μM caffeine to HEK-RyR1 cells pretreated with 0.1–10 μM o,p'-DDT (triangle trace), p,p'-DDT (inverted triangle traces), o,p'-DDE (circle traces), or p,p'-DDE (square traces) or 0.1% DMSO (v/v) vehicle control. The (B) amplitude and (C) under the curve (AUC) of the caffeine response were quantified and plotted for each concentration of DDT or DDE. Experiments were performed in triplicate and repeated 4 times (n = 4).

in male rats due to reciprocal interaction of the estrogen receptor-alpha (ESRα) with RyRs (Ferrari et al., 2016; Khomula et al., 2017). There are numerous recognized post-translational RyR modifications, such as S-nitrosylation and S-palmitoylation, that are known to modulate the activity and/or sensitivity of RyR (Bellinger et al., 2009; Chaube et al., 2014; Lanner et al., 2010; Witherspoon and Meilleur, 2016). RyR1 is also tightly regulated by cellular redox state (Aracena et al., 2005; Feng et al., 2000; Xia et al., 2000), a physiological property conferring sensitivity to redox-active xenobiotics, such as anthraquinones and naphthoquinones. Aging and muscle wasting diseases produce similar pathological changes in skeletal muscle of both sexes, including increased oxidative stress, mitochondrial dysfunction, inflammation, satellite cell senescence, and apoptosis (Anderson et al., 2017). However, age- and/or disease-induced alterations in sex hormones are major contributors to muscle wasting, and hence males and females may respond differently to DDx due to their unique hormonal profiles. Moreover, sex differences in the level of skeletal muscle oxidative stress, such as those recently reported to occur after eccentric exercise indicate women respond with accentuated impaired redox balance compared with men (Wiecek et al., 2017). Thus, it is possible, and more than likely, that differences in the level or the type of post-translational modification may be different between skeletal muscle in males and in females, which may contribute to sex-differences in susceptibility to DDx exposure. We posit that differential post-translational modification of RyR1 in the 2 sexes prior to collection of skeletal muscle tissue, such as those mediated by activation of ESRα, may have contributed to the observed significant sex differences in the efficacy of DDx. In support of this hypothesis, western blot analysis showed no differences in RyR1 protein expression between preparations from females and males. However, further studies are needed to compare the differential post-translational modification of RyR1 in skeletal muscle of males versus females, and how these differences contribute to sex-differences in RyR1 sensitivity (conformation) and/or function.
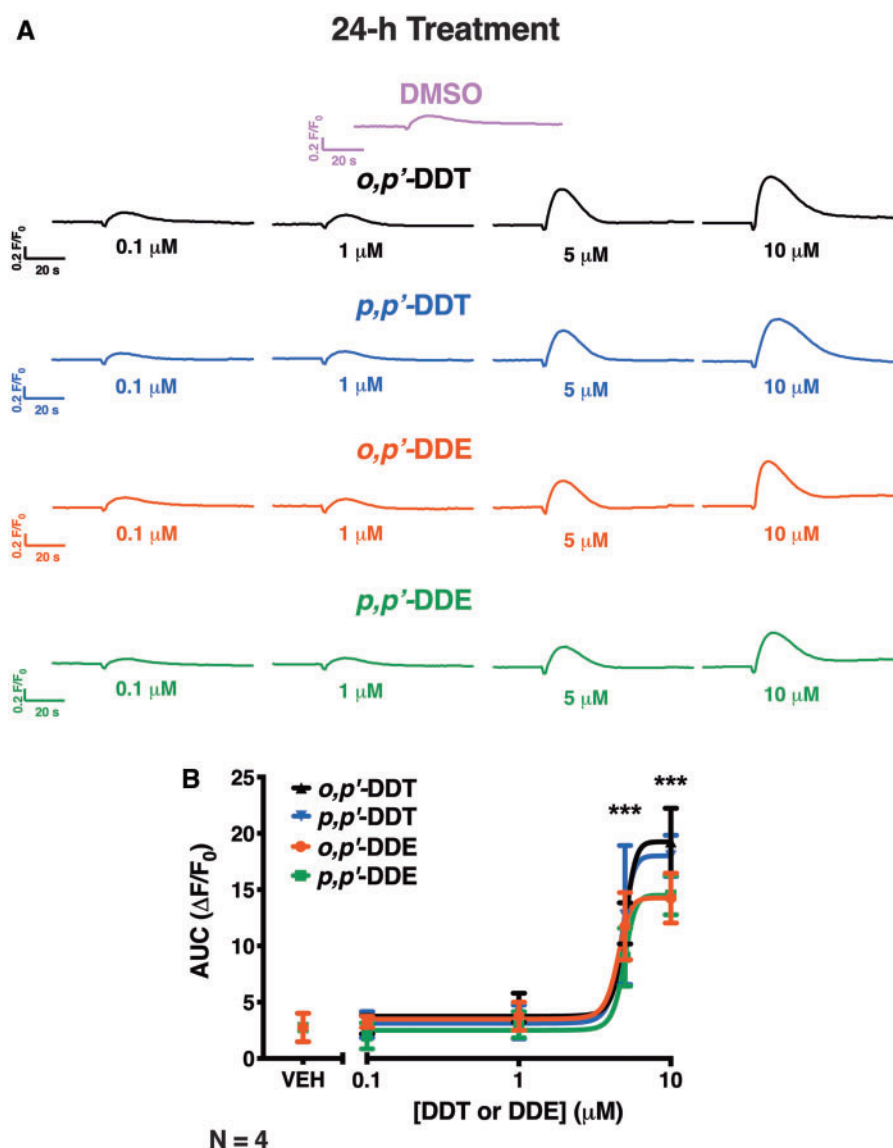
Figure 9. Pretreatment of HEK-RyR1 cells for 24 h with increasing concentrations of dichlorodiphenyltrichloroethane (DDT) or dichlorodiphenyldichloroethylene (DDE) congeners sensitized HEK-RyR1 cells to caffeine in a dose-dependent manner. (A) Ca^{2+}-transient response mediated by addition of 100 μM caffeine to HEK-RyR1 cells pretreated with 0.1–10 μM o,p'-DDT (triangle trace), p,p'-DDT (inverted triangle traces), o,p'-DDE (circle traces), or p,p'-DDE (square traces) or 0.1% DMSO (v/v) vehicle control for 24 h. (B), The area under the curve (AUC) of each trace response were quantified and plotted across all concentrations of DDT and DDE. The analysis of the amplitude of each trace was identical to the AUC (not shown). All DDT and DDE congeners at 5 μM and 10 μM drastically sensitized RyR1 to the activating effect of caffeine and, thus significantly increased amplitude and AUC (***$p < .001$). Experiments were performed in triplicate and repeated 4 times ($n = 4$). Statistical comparison of the effect of DDT and DDE congeners to DMSO vehicle control was performed with a one-way ANOVA with Dunnett *post hoc* test.

Although we show that 10 μM DDx is capable of rapidly triggering Ca^{2+} release from JSR vesicles by an RyR1 mechanism, it produces more complex responses in intact human embryonic kidney cells expressing RyR1 (HEK-RyR1) and in skeletal myotubes. Acute exposure to DDx did not cause an immediate rise in cytoplasmic Ca^{2+}, which is most likely due to RyR1 not being readily accessible; DDx would require time to penetrate the cell membrane to reach the intracellular target. In support of this hypothesis, pretreatment with DDx ranging from 100 s to 24 h, significantly increased RyR1 sensitivity to activation by agonist, caffeine. The longer HEK-RyR1 cells were pretreated with DDx the more DDx sensitized RyR1 to activation, significantly enhancing the amplitude and/or the AUC of the caffeine-induced Ca^{2+} release compared with vehicle control. A similar phenomenon was observed with primary mouse myotubes, where

pretreatment with o,p'-DDE for 24 h heightened myotube responses to electrical stimuli across the entire frequency range applied in this study.

To our knowledge, this is the first demonstration that DDx has the potential to affect muscle health through interaction with a component of the ECC machinery, RyR1. The 4 DDx are not only capable of directly interacting with RyR1, but they are also efficacious activators of the receptor and strongly sensitize it to activation by agonists in intact cells and skeletal myotubes. Alterations in RyR1 function, including hyper-sensitization of RyR1, increasing its open probability or prolonging open time by agonists, can lead to abnormal Ca^{2+} dysregulation in skeletal muscle, and ultimately, symptoms of muscle impairment and myopathy such as muscle weakness (Dulhunty *et al.*, 2017; Gehlert *et al.*, 2015; Laughlin *et al.*, 2017; Vallejo-Illarramendi
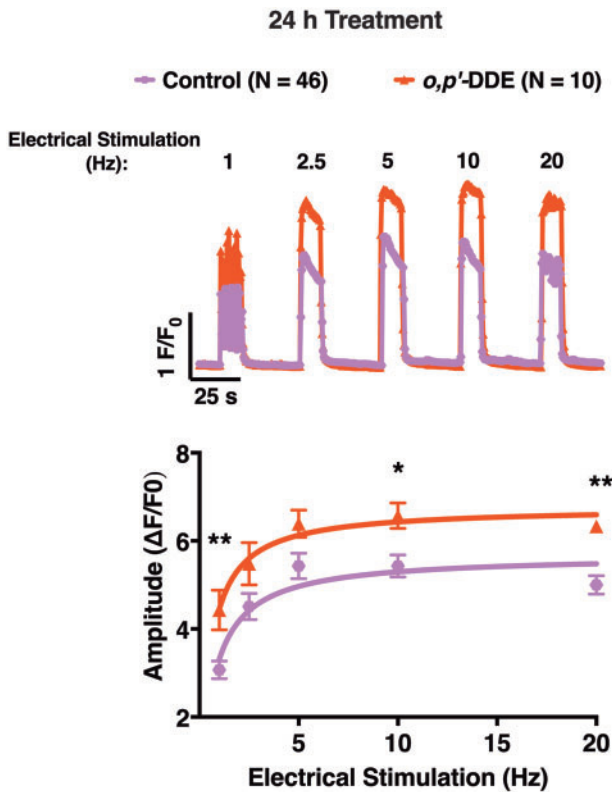
Figure 10. Differentiated myotubes pretreated with 1 μM o,p'-DDE for 24h exhibited heightened sensitivity to electrical stimulation compared with DMSO vehicle control-treated myotubes. Representative traces of the Ca^{2+}-transient response mediated by increasing electrical stimulation frequency applied to myotubes pretreated with either 1 μM o,p'-DDE or 0.01% DMSO (v/v) vehicle control. The amplitude of the Ca^{2+} transients of o, p'-DDE pretreated cells (triangle trace) and vehicle pretreated cells (hexagon trace) were quantified and plotted across all electrical stimulation frequency, and a Student's t-test was performed to determine statistical significance between the 2 groups (*$p < .05$; **$p < .01$). Myotubes pretreated with o,p'-DDE displayed greater Ca^{2+}-transient amplitudes across all electrical stimulation frequencies compared with vehicle control pretreated cells. Experiments were replicated at least twice using 2 different passages, and all responding control cells ($N = 46$) and o,p'-DDE pretreated cells ($N = 10$) were used for analysis. Data shown represent the mean ± SEM.

et al., 2014). Abnormal regulation of RyR1 modulation, especially physiological, xenobiotic, and/or physical stressors that sensitize its channel activity (ie produce a net gain-of-function), as in the case of RyR1 mutations that cause malignant hyperthermia, are a common cause of exertional rhabdomyolysis in otherwise healthy individuals (Voermans et al., 2016). RyR1-related myopathies in humans can also cause muscle injury, fatigue, and weakness overtime (Witherspoon et al., 2018), which may be an implication of DDx. Exposure to o,p'-DDE did not only sensitize myotubes to electrical stimulation, but it also produced abnormal patterns in fatigability. Currently, numerous RyR1 congenital myopathies, that typically confer a gain-of-function, have been identified (Lawal et al., 2018; Witherspoon and Meilleur, 2016), and they are well known to cause clinical neuromuscular issues. DDx has also been shown to impair myogenesis dose- and time-dependently (Kim et al., 2017), and this in combination with its ability to modulate RyR1 activity to cause Ca^{2+} dysregulation in muscle cells can lead to exacerbation of muscle impairments in not only populations with RyR1 congenital myopathies, but also in healthy individuals. Therefore, further

studies are warranted to investigate how DDx differentially affects both population of individuals.

Significant sensitization of RyR1 in our cell-based in vitro assay necessitated 5–10 μM of DDT to facilitate subchronic and chronic impairments in RyR1 channel function and associated changes in Ca^{2+} dynamics in cells; although our Ca^{2+} imaging experiments with myotubes suggests that lower concentrations (nanomolar range) are sufficient to facilitate muscle dysfunction, because the 1 μM o,p'-DDE pretreatment was performed in the presence of 5% serum and DDx is undoubtedly highly protein bound. The high concentration membrane lipid present in microsomal [^{3}H]Ry-binding assays and the incubation conditions are likely contributors to a lower apparent potency of highly lipophilic xenobiotic molecules due to partitioning in the lipid phase, as previously demonstrated with single channel voltage clamp studies with PCB congeners (Holland et al., 2017). Monolayers of myotubes proved to be a very sensitive model to o,p'-DDE, eliciting abnormal ECC and fatigability at low micromolar exposures, revealing that ECC may be a particularly sensitive target to DDx. More importantly, a much lower concentration may be sufficient to cause muscle impairment in the case of chronic exposure. An epidemiological study with chronically exposed DDT workers concluded that they suffered a significant permanent decline in their motor skills (ie grip strength and reaction time), where severity of decline was associated with years of DDT exposure (van Wendel de Joode et al., 2001). The study supports the hypothesis that muscle impairment and myopathy may occur with prolonged DDT exposure, and our cumulative data suggest this may be due to DDx acting on RyR1 over time.

Moreover, chronic exposure permits a continuous increase in DDT body burden over time, which poses a second potential consequence. Although DDT, like other organochlorines, is typically sequestered in adipose tissue in mammals, it is also distributed to various organs such as the brain, thymus, testis, kidney, liver, and muscle (Tebourbi et al., 2006; Zitko et al., 1998). During periods of increased activity/energy expenditure or starvation in mammals, DDT is redistributed to various organs and the concentration of DDT in blood plasma increases (Dale et al., 1962; Findlay and DeFreitas, 1971), which may steadily expose highly perfused organs such as skeletal muscle to DDT. As aforementioned, skeletal muscle is one of organs that DDT initially distributes to, so introduction of increased DDT exposure in plasma during periods of energy expenditure would not only increase the chemical concentration at the site of action, but it may increase the concentration sufficiently enough to accelerate muscle impairments and/or function. Because DDT is still used in numerous countries around the world to control against vector-borne diseases and it is still detected in the tissues of individuals in areas where it has been banned or restricted for decades, functional studies are needed to determine what myopathies DDx may ultimately confer.

SUPPLEMENTARY DATA

Supplementary data are available at Toxicological Sciences online.

ACKNOWLEDGMENT

DECLARATION OF CONFLICTING INTERESTS

The authors declared no potential conflicts of interest with respect to the research, authorship, and/or publication of this article.

REFERENCES

Anderson, L. J., Liu, H., and Garcia, J. M. (2017). Sex differences in muscle wasting. *Adv. Exp. Med. Biol.* **1043**, 153–197.

Aracena, P., Tang, W., Hamilton, S. L., and Hidalgo, C. (2005). Effects of S-glutathionylation and S-nitrosylation on calmodulin binding to triads and FKBP12 binding to type 1 calcium release channels. *Antioxid. Redox Signal.* **7**, 870–881.

Baker, M. E., and Lathe, R. (2018). The promiscuous estrogen receptor: Evolution of physiological estrogens and response to phytochemicals and endocrine disruptors. *J. Steroid Biochem. Mol. Biol.* **184**, 29–37.

Barrientos, G., Bose, D. D., Feng, W., Padilla, I., and Pessah, I. N. (2009). The $Na+/Ca^{2+}$ exchange inhibitor 2-(2-(4-(4-nitrobenzyloxy)phenyl)ethyl)isothiourea methanesulfonate (KB-R7943) also blocks ryanodine receptors type 1 (RyR1) and type 2 (RyR2) channels. *Mol. Pharmacol.* **76**, 560–568.

Bellinger, A. M., Mongillo, M., and Marks, A. R. (2008). Stressed out: The skeletal muscle ryanodine receptor as a target of stress. *J. Clin. Invest.* **118**, 445–453.

Bellinger, A. M., Reiken, S., Carlson, C., Mongillo, M., Liu, X., Rothman, L., Matecki, S., Lacampagne, A., and Marks, A. R. (2009). Hypernitrosylated ryanodine receptor calcium release channels are leaky in dystrophic muscle. *Nat. Med.* **15**, 325–330.

Bornman, M., Delport, R., Farías, P., Aneck-Hahn, N., Patrick, S., Millar, R. P., and de Jager, C. (2018). Alterations in male reproductive hormones in relation to environmental DDT exposure. *Environ. Int.* **113**, 281–289.

Chaube, R., Hess, D. T., Wang, Y.-J., Plummer, B., Sun, Q.-A., Laurita, K., and Stamler, J. S. (2014). Regulation of the skeletal muscle ryanodine receptor/Ca^{2+}-release channel RyR1 by S-palmitoylation. *J. Biol. Chem.* **289**, 8612–8619.

Cherednichenko, G., Ward, C. W., Feng, W., Cabrales, E., Michaelson, L., Samso, M., Lopez, J. R., Allen, P. D., and Pessah, I. N. (2008). Enhanced excitation-coupled calcium entry in myotubes expressing malignant hyperthermia mutation R163C is attenuated by dantrolene. *Mol. Pharmacol.* **73**, 1203–1212.

Cherednichenko, G., Zhang, R., Bannister, R. A., Timofeyev, V., Li, N., Fritsch, E. B., Feng, W., Barrientos, G. C., Schebb, N. H., and Hammock, B. D. (2012). Triclosan impairs excitation-contraction coupling and Ca^{2+} dynamics in striated muscle. *Proc. Natl. Acad. Sci. U.S.A.* **109**, 14158–14163.

Coats, J. R. (1990). Mechanisms of toxic action and structure-activity relationships for organochlorine and synthetic pyrethroid insecticides. *Environ. Health Perspect.* **87**, 255–262.

Coffin, S., Gan, J., and Schlenk, D. (2017). Comparisons of field and laboratory estimates of risk of DDTs from contaminated sediments to humans that consume fish in Palos Verdes, California, USA. *Sci. Total Environ.* **601–602**, 1139–1146.

Dale, W. E., Gaines, T. B., and Hayes, W. J., Jr (1962). Storage and excretion of DDT in starved rats. *Toxicol. Appl. Pharmacol.* **4**, 89–106.

Dulhunty, A. F., Board, P. G., Beard, N. A., and Casarotto, M. G. (2017). Physiology and pharmacology of ryanodine receptor calcium release channels. *Adv. Pharmacol.* **79**, 287–324.

EPA. (2017) DDT—a brief history and status. In (EPA, Ed.). World Health Organization. https://www.epa.gov/ingredients-used-pesticide-products/ddt-brief-history-and-status. Accessed January 1, 2019.

Feng, W., Liu, G., Allen, P. D., and Pessah, I. N. (2000). Transmembrane redox sensor of ryanodine receptor complex. *J. Biol. Chem.* **275**, 35902–35907.

Feng, W., Zheng, J., Robin, G., Dong, Y., Ichikawa, M., Inoue, Y., Mori, T., Nakano, T., and Pessah, I. N. (2017). Enantioselectivity of 2,2′,3,5′,6-pentachlorobiphenyl (PCB 95) atropisomers toward ryanodine receptors (RyRs) and their influences on hippocampal neuronal networks. *Environ. Sci. Technol.* **51**, 14406–14416.

Ferrari, L. F., Khomula, E. V., Araldi, D., and Levine, J. D. (2016). Marked sexual dimorphism in the role of the ryanodine receptor in a model of pain chronification in the rat. *Sci. Rep.* **6**, 31221.

Findlay, G. M., and DeFreitas, A. S. (1971). DDT movement from adipocyte to muscle cell during lipid utilization. *Nature* **229**, 63–65.

Gach, M. P., Cherednichenko, G., Haarmann, C., Lopez, J. R., Beam, K. G., Pessah, I. N., Franzini-Armstrong, C., and Allen, P. D. (2008). Alpha2delta1 dihydropyridine receptor subunit is a critical element for excitation-coupled calcium entry but not for formation of tetrads in skeletal myotubes. *Biophys. J.* **94**, 3023–3034.

Gehlert, S., Bloch, W., and Suhr, F. (2015). Ca^{2+}-dependent regulations and signaling in skeletal muscle: From electro-mechanical coupling to adaptation. *Int. J. Mol. Sci.* **16**, 1066–1095.

Gellert, R. J., Heinrichs, W. L., and Swerdloff, R. S. (1972). DDT homologues: Estrogen-like effects on the vagina, uterus and pituitary of the rat. *Endocrinology* **91**, 1095–1100.

Holland, E. B., Feng, W., Zheng, J., Dong, Y., Li, X., Lehmler, H.-J., and Pessah, I. N. (2017). An extended structure-activity relationship of nondioxin-like PCBs evaluates and supports modeling predictions and identifies picomolar potency of PCB 202 towards ryanodine receptors. *Toxicol. Sci.* **155**, 170–181.

Jones, J. L., Reynolds, D. F., Lai, F. A., and Blayney, L. M. (2005). Ryanodine receptor binding to FKBP12 is modulated by channel activation state. *J. Cell Sci.* **118**, 4613–4619.

Kelce, W. R., Stone, C. R., Laws, S. C., Gray, L. E., Kemppainen, J. A., and Wilson, E. M. (1995). Persistent DDT metabolite *p,p′*-DDE is a potent androgen receptor antagonist. *Nature* **375**, 581–585.

Khomula, E. V., Ferrari, L. F., Araldi, D., and Levine, J. D. (2017). Sexual dimorphism in a reciprocal interaction of ryanodine and IP3 receptors in the induction of hyperalgesic priming. *J. Neurosci.* **37**, 2032–2044.

Kim, J., Park, M. Y., Kim, Y., Yoon, K. S., Clark, J. M., Park, Y., and Whang, K.-Y. (2017). 4,4′-Dichlorodiphenyltrichloroethane (DDT) and 4,4′-dichlorodiphenyldichloroethylene (DDE) inhibit myogenesis in C2C12 myoblasts. *J. Sci. Food Agric.* **97**, 5176–5185.

Kim, K. H., Bose, D. D., Ghogha, A., Riehl, J., Zhang, R., Barnhart, C. D., Lein, P. J., and Pessah, I. N. (2011). Para- and ortho-substitutions are key determinants of polybrominated

diphenyl ether activity toward ryanodine receptors and neurotoxicity. *Environ. Health Perspect.* **119**, 519–526.

Kojima, H., Katsura, E., Takeuchi, S., Niiyama, K., and Kobayashi, K. (2004). Screening for estrogen and androgen receptor activities in 200 pesticides by *in vitro* reporter gene assays using Chinese hamster ovary cells. *Environ. Health Perspect.* **112**, 524–531.

Kucher, S., and Schwarzbauer, J. (2017). DDT-related compounds as non-extractable residues in submarine sediments of the Palos Verdes Shelf, California, USA. *Chemosphere* **185**, 529–538.

Lanner, J. T., Georgiou, D. K., Joshi, A. D., and Hamilton, S. L. (2010). Ryanodine receptors: Structure, expression, molecular details, and function in calcium release. *Cold Spring Harb. Perspect. Biol.* **2**, a003996.

Laughlin, R. S., Niu, Z., Wieben, E., and Milone, M. (2017). RYR1 causing distal myopathy. *Mol. Genet. Genomic Med.* **5**, 800–804.

Lawal, T. A., Todd, J. J., and Meilleur, K. G. (2018). Ryanodine receptor 1-related myopathies: Diagnostic and therapeutic approaches. *Neurotherapeutics* **115**, 885–899.

Mansouri, A., Cregut, M., Abbes, C., Durand, M. J., Landoulsi, A., and Thouand, G. (2017). The environmental issues of DDT pollution and bioremediation: A multidisciplinary review. *Appl. Biochem. Biotechnol.* **181**, 309–339.

Mendes, R. A., Lopes, A. S., de Souza, L. C., Lima, M. O., and Santos, L. S. (2016). DDT concentration in fish from the Tapajos River in the Amazon region, Brazil. *Chemosphere* **153**, 340–345.

Mnif, W., Hassine, A. I., Bouaziz, A., Bartegi, A., Thomas, O., and Roig, B. (2011). Effect of endocrine disruptor pesticides: A review. *Int. J. Environ. Res. Public Health* **8**, 2265–2303.

Morisseau, C., Merzlikin, O., Lin, A., He, G., Feng, W., Padilla, I., Denison, M. S., Pessah, I. N., and Hammock, B. D. (2009). Toxicology in the fast lane: Application of high-throughput bioassays to detect modulation of key enzymes and receptors. *Environ. Health Perspect.* **117**, 1867–1872.

Narahashi, T. (2000). Neuroreceptors and ion channels as the basis for drug action: Past, present, and future. *J. Pharmacol. Exp. Ther.* **294**, 1–26.

Nicolopoulou-Stamati, P., Maipas, S., Kotampasi, C., Stamatis, P., and Hens, L. (2016). Chemical pesticides and human health: The urgent need for a new concept in agriculture. *Front. Public Health* **4**, 148.

Niknam, Y., Feng, W., Cherednichenko, G., Dong, Y., Joshi, S. N., Vyas, S. M., Lehmler, H.-J., and Pessah, I. N. (2013). Structure-activity relationship of selected meta- and para-hydroxylated non-dioxin like polychlorinated biphenyls: From single RyR1 channels to muscle dysfunction. *Toxicol. Sci.* **136**, 500–513.

Ozawa, T. (2010). Modulation of ryanodine receptor Ca^{2+} channels (review). *Mol. Med. Rep.* **3**, 199–204.

Patrick, S. M., Bornman, M. S., Joubert, A. M., Pitts, N., Naidoo, V., and de Jager, C. (2016). Effects of environmental endocrine disruptors, including insecticides used for malaria vector control on reproductive parameters of male rats. *Reprod. Toxicol.* **61**, 19–27.

Patterson, D. G., Wong, L.-Y., Turner, W. E., Caudill, S. P., Dipietro, E. S., McClure, P. C., Cash, T. P., Osterloh, J. D., Pirkle, J. L., Sampson, E. J., *et al.* (2009). Levels in the U.S. population of those persistent organic pollutants (2003–2004) included in the Stockholm Convention or in other long range transboundary air pollution agreements. *Environ. Sci. Technol.* **43**, 1211–1218.

Pessah, I. N., Anderson, K. W., and Casida, J. E. (1986). Solubilization and separation of Ca^{2+}-ATPase from the Ca^{2+}-ryanodine receptor complex. *Biochem. Biophys. Res. Commun.* **139**, 235–243.

Pessah, I. N., Cherednichenko, G., and Lein, P. J. (2010). Minding the calcium store: Ryanodine receptor activation as a convergent mechanism of PCB toxicity. *Pharmacol. Ther.* **125**, 260–285.

Pessah, I. N., Lehmler, H.-J., Robertson, L. W., Perez, C. F., Cabrales, E., Bose, D. D., and Feng, W. (2009). Enantiomeric specificity of (−)-2,2′,3,3′,6,6′-hexachlorobiphenyl toward ryanodine receptor types 1 and 2. *Chem. Res. Toxicol.* **22**, 201–207.

Pessah, I. N., and Zimanyi, I. (1991). Characterization of multiple [3H]ryanodine binding sites on the Ca^{2+} release channel of sarcoplasmic reticulum from skeletal and cardiac muscle: Evidence for a sequential mechanism in ryanodine action. *Mol. Pharmacol.* **39**, 679–689.

Rodriguez-Alcala, L. M., Sa, C., Pimentel, L. L., Pestana, D., Teixeira, D., Faria, A., Calhau, C., and Gomes, A. (2015). Endocrine disruptor DDE associated with a high-fat diet enhances the impairment of liver fatty acid composition in rats. *J. Agric. Food Chem.* **63**, 9341–9348.

Saito, A., Seiler, S., Chu, A., and Fleischer, S. (1984). Preparation and morphology of sarcoplasmic reticulum terminal cisternae from rabbit skeletal muscle. *J. Cell Biol.* **99**, 875–885.

Sanger, D. M., Holland, A. F., and Scott, G. I. (1999). Tidal creek and salt marsh sediments in South Carolina coastal estuaries: II. Distribution of organic contaminants. *Arch. Environ. Contam. Toxicol.* **37**, 458–471.

Silver, K., Dong, K., and Zhorov, B. S. (2017). Molecular mechanism of action and selectivity of sodium channel blocker insecticides. *Curr. Med. Chem.* **24**, 2912–2924.

Snoeck, M., van Engelen, B. G. M., Küsters, B., Lammens, M., Meijer, R., Molenaar, J. P. F., Raaphorst, J., Verschuuren-Bemelmans, C. C., Straathof, C. S. M., Sie, L. T. L., *et al.* (2015). RYR1-related myopathies: A wide spectrum of phenotypes throughout life. *Eur. J. Neurol.* **22**, 1094.

Tebourbi, O., Driss, M. R., Sakly, M., and Rhouma, K. B. (2006). Metabolism of DDT in different tissues of young rats. *J. Environ. Sci. Health B* **41**, 167–176.

Truong, K. M., and Pessah, I. N. (2018). Comparison of chlorantraniliprole and flubendiamide activity towards wild type and malignant hyperthermia-susceptible ryanodine receptors and heat stress intolerance. *Toxicol. Sci* **167**, 509–523.

Turusov, V., Rakitsky, V., and Tomatis, L. (2002). Dichlorodiphenyltrichloroethane (DDT): Ubiquity, persistence, and risks. *Environ. Health Perspect.* **110**, 125–128.

Tyagi, V., Garg, N., Mustafa, M. D., Banerjee, B. D., and Guleria, K. (2015). Organochlorine pesticide levels in maternal blood and placental tissue with reference to preterm birth: A recent trend in North Indian population. *Environ. Monit. Assess.* **187**, 471.

Vallejo-Illarramendi, A., Toral-Ojeda, I., Aldanondo, G., and Lopez de Munain, A. (2014). Dysregulation of calcium homeostasis in muscular dystrophies. *Expert Rev. Mol. Med.* **16**, e16.

van den Berg, H., Manuweera, G., and Konradsen, F. (2017). Global trends in the production and use of DDT for control of malaria and other vector-borne diseases. *Malar. J.* **16**, 401.

van Wendel de Joode, B., Wesseling, C., Kromhout, H., Monge, P., Garcia, M., and Mergler, D. (2001). Chronic nervous-system effects of long-term occupational exposure to DDT. *Lancet* **357**, 1014–1016.

Voermans, N. C., Snoeck, M., and Jungbluth, H. (2016). RYR1-related rhabdomyolysis: A common but probably underdiagnosed manifestation of skeletal muscle ryanodine receptor dysfunction. *Rev. Neurol. (Paris)* **172**, 546–558.

Wiecek, M., Maciejczyk, M., Szymura, J., and Szygula, Z. (2017). Sex differences in oxidative stress after eccentric and concentric exercise. *Redox Rep.* **22**, 478–485.

Witherspoon, J. W., and Meilleur, K. G. (2016). Review of RyR1 pathway and associated pathomechanisms. *Acta Neuropathol. Commun.* **4**, 121.

Witherspoon, J. W., Vasavada, R. P., Waite, M. R., Shelton, M., Chrismer, I. C., Wakim, P. G., Jain, M. S., Bonnemann, C. G., and Meilleur, K. G. (2018). 6-Minute walk test as a measure of disease progression and fatigability in a cohort of individuals with RYR1-related myopathies. *Orphanet J. Rare Dis.* **13**, 105.

Xia, R., Stangler, T., and Abramson, J. J. (2000). Skeletal muscle ryanodine receptor is a redox sensor with a well defined redox potential that is sensitive to channel modulators. *J. Biol. Chem.* **275**, 36556–36561.

Zhang, R., and Pessah, I. N. (2017). Divergent mechanisms leading to signaling dysfunction in embryonic muscle by bisphenol A and tetrabromobisphenol A. *Mol. Pharmacol.* **91**, 428–436.

Zhorov, B. S., and Dong, K. (2017). Elucidation of pyrethroid and DDT receptor sites in the voltage-gated sodium channel. *Neurotoxicology* **60**, 171–177.

Zitko, V., Stenson, G., and Hellou, J. (1998). Levels of organochlorine and polycyclic aromatic compounds in harp seal beaters (*Phoca groenlandica*). *Sci. Total Environ.* **221**, 11–29.

Zumbado, M., Goethals, M., Álvarez-León, E. E., Luzardo, O. P., Cabrera, F., Serra-Majem, L., and Domínguez-Boada, L. (2005). Inadvertent exposure to organochlorine pesticides DDT and derivatives in people from the Canary Islands (Spain). *Sci. Total Environ.* **339**, 49–62.